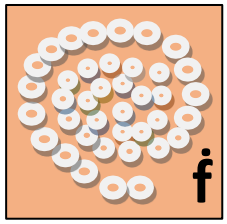

International Journal of Mathematical Analysis and Modelling

(Formerly Journal of the Nigerian Society for Mathematical Biology)

Volume 9 Issue 1 (June), 2026

ISSN (Print): 2682 - 5694
ISSN (Online): 2682 – 5708
www.tnsmb.org

A mathematical model to assess the impact of asymptomatic infections on Malaria transmission dynamics incorporating awareness campaigns and treatment

Abimbola Abolarinwa*, **Isaac O. Olusola**†, and **Gbeminiyi J. Oyedele**‡

Abstract

Malaria transmission in sub-Saharan Africa is sustained in part by a large reservoir of asymptomatic infections that perpetuate transmission. While awareness-based interventions are widely promoted to improve prevention and treatment-seeking behaviour, their interaction with asymptomatic transmission is rarely examined. We develop a deterministic compartmental model that integrates awareness stratification of susceptible individuals with explicit compartments for asymptomatic, symptomatic, treated, and recovered humans, coupled with a vector population. Susceptible individuals are classified into low- and high-awareness groups, with transitions governed by awareness campaigns and waning awareness. The basic reproduction number is derived using the next-generation matrix method, and conditions for local and global stability of the malaria-free equilibrium are established. Sensitivity analysis identifies key parameters influencing transmission dynamics. The quantitative result of the threshold R_0 reveals that asymptomatic cases contribute approximately 90.7% to the basic reproduction number, while symptomatic cases account for about 9.3%. The result also shows that awareness alone is insufficient for malaria elimination in the presence of a substantial asymptomatic reservoir. However, combined strategies incorporating enhanced awareness, increased treatment coverage, reduced vector-human contact, and detection of asymptomatic infections significantly reduce transmission. The model underscores the need to integrate behavioural interventions with strategies targeting hidden infections to support malaria elimination efforts.

Keywords and phrases: asymptomatic infection; Malaria; transmission dynamics; treatment; sensitivity analysis; stability analysis

1 Introduction

Malaria remains one of the most persistent infectious diseases globally, with sub-Saharan Africa bearing over 95% of the burden. WHO estimates show 263 million cases and 597,000 deaths in 2023, with children under five and pregnant women especially vulnerable [1]. A major obstacle to elimination is the high prevalence of asymptomatic infections, which act as silent reservoirs of *Plasmodium falciparum*. Studies report asymptomatic parasitemia of 34–35% in Ugandan children, 6–11% among Ethiopian pregnant women, and nearly 19% in parts of Nigeria [2].

Our investigation into modelling studies highlights the epidemiological importance of these hidden infections. Haringo et al. [2] showed that asymptomatic carriers contribute about 30% of the basic reproduction number, R_0, and can lead to backward bifurcation, whereby malaria persists even when $R_0 < 1$. Haile et al. [3] found that parameters governing unrecognized infections strongly influence R_0, emphasizing the role of hidden transmission. Xue et al. [4] demonstrated that including

*Corresponding Author; E-mail: aabolarinwa@unilag.edu.ng; Department of Mathematics, University of Lagos, Akoka, Lagos, Nigeria

†Department of Mathematics, University of Ibadan, Ibadan, Nigeria; E-mail: ziglaginstitute@gmail.com

‡Warwick Medical School, University of Warwick, Coventry, United Kingdom; E-mail: Gbeminiyi.Oyedele@warwick.ac.uk

an asymptomatic class markedly alters equilibrium behavior and that models ignoring such carriers underestimate long-term prevalence. Jaleta et al. [5] further showed that interventions targeting both symptomatic and asymptomatic infections—particularly active screening and treatment—substantially outperform symptomatic-only strategies. Empirical findings support these conclusions: Rek et al. [6] reported that asymptomatic and submicroscopic infections accounted for up to 95% of the infectious reservoir among school-aged children, while Mandai et al. [7] identified high asymptomatic prevalence driven by age, exposure, and LLIN use.

In addition, research underscores the importance of awareness-based behavioural interventions. Models by Collins and Duffy [8] and Adegbite et al. [9] incorporate treatment access, immunity, mobility, and preventive practices. Awareness models from Al Basir and Abraha [10] and Ochieng [11] demonstrate that education and media campaigns can enhance preventive behavior and reduce infection prevalence. More recently, Haringo et al. [12] included awareness programmes, insecticide use, and treatment uptake, reinforcing the value of behavioural dynamics in malaria control.

Despite these advances, most awareness-based models do not distinguish between symptomatic and asymptomatic infections, while models focused on asymptomatic dynamics often ignore behavioural influences. This disconnect limits the ability to evaluate how awareness interacts with hidden infection reservoirs.

To bridge this gap, we propose a deterministic compartmental model, motivated by the work of Haringo et al. [12, 2]. The model integrates awareness-stratified susceptibility with an explicit asymptomatic infectious class, alongside symptomatic, treated, and recovered compartments, and a full mosquito system. Awareness influences preventive behaviour and treatment-seeking, while asymptomatic individuals contribute significantly to transmission and may progress to symptomatic disease. This integrated structure enables evaluation of how behavioural changes, treatment coverage, and hidden reservoirs interact to shape malaria dynamics. Our analysis shows that although awareness reduces risky behaviour, it is insufficient when asymptomatic prevalence is high; combining awareness with interventions targeting asymptomatic detection and vector control yields the strongest reductions in transmission.

The remainder of this paper is structured as follows: Section 2 presents the model formulation and assumptions; Section 3 provides analytical results including equilibria, the basic reproduction number, and stability; Section 4 discusses sensitivity analyses and numerical simulations; and Section 5 summarizes findings, policy implications, and directions for future research.

2 Methodology/Model Formulation

This study aims to address some of the gaps in malaria awareness models and the role of awareness campaigns in reducing the pool of asymptomatic individuals in a population. This study presents a compartmental, deterministic system of ordinary differential equations designed to simulate the transmission dynamics of malaria in a human population with varying risk and a mosquito vector population.

We assume that the susceptible individuals are divided into two groups based on their level of awareness of the infection: the high risk (low level of awareness), S_1, and the low risk (high level of awareness), S_2. The S_1 class is educated at the per capita rate ρ and thereafter moves into the S_2 class (representing the adoption of bed net interventions, indoor residual spraying, or other protective measures). Malaria infection can invade the S_1 and S_2 classes depending on the rate of bite prevention of the mosquitoes with the use of Long-Lasting Insecticidal Nets (LLINs). The awareness program is assumed to reduce the likelihood of infection by providing sustainable LLIN or a guide to effective Indoor Residual Spraying (IRS), which is measured by a factor of α_3 ($0 \leq \alpha_3 \leq 1$). The case where $\alpha_3 = 0$ signifies a completely effective program, while $\alpha_3 = 1$ models the situation where the program is totally ineffective.

It was further taken into consideration that the education program produces temporary protective behavior which wanes at the per capita rate θ. A rate of $\theta \to \infty$ corresponds to the case where there is absolutely no retention of awareness, while $\theta = 0$ indicates life-long adherence to protective behaviors.

Hence, θ measures the rate at which those in the S_2 class return to the S_1 class due to forgetfulness or fatigue. We define our transmission probability for the human population as β_h and for the mosquito population as β_m.

The variables $E_h, A_h, I_h, T_h,$ and R_h represent the human compartments of exposed, asymptomatic infected, symptomatic infected, treated, and recovered individuals, while the variables $S_m, E_m,$ and I_m represent the susceptible, exposed, and infectious mosquito compartments. Exposed individuals can move back to the susceptible class at the rate of k due to immunological clearance of pre-erythrocytic stages [11]. The fraction of exposed individuals who revert to the high-risk susceptible class (S_1) due to robust immune clearance is given as z, and the remaining fraction $(1-z)$ reverts to the low-risk susceptible class (S_2) [11]. The recruitment rate for the human and vector populations is given by Λ_h and Λ_m, respectively.

After the incubation period, exposed individuals progress to become infectious (either asymptomatic or symptomatic) at the per capita rate γ_h. The fraction of individuals who develop clinical symptoms directly after the incubation period is given by Φ $(0 < \Phi < 1)$, and the remaining fraction $1-\Phi$ enter the asymptomatic carrier class. Asymptomatic individuals can clinically progress to the symptomatic class upon developing symptoms or recover due to screening followed by on-spot treatment tactic [2]. The progression rate from the asymptomatic to symptomatic class is denoted by ω, and the fraction of progressing asymptomatic carriers who become clinically symptomatic is given by χ $(0 < \chi < 1)$. Symptomatic individuals are treated at the per capita rate ξ (e.g., using artemisinin-based combination therapies, ACTs) to move to the treated class. Treated individuals can die due to treatment failure or severe complications at the rate α_1, and recover at the rate τ to move to the recovered class. Recovered individuals lose temporary immunity and return to the susceptible class at the rate σ. The proportion of recovered individuals who return to the low-risk susceptible class (S_2) is given by q, while the remaining fraction $1-q$ return to the high-risk class S_1.

The parameter α_2 $(0 \leq \alpha_2 \leq 1)$ represents the relative infectiousness of symptomatic individuals compared to asymptomatic carriers. μ_h and μ_m represent the natural death rates of the human and mosquito populations, respectively. The rate at which exposed mosquitoes become infectious and move to the infected vector class I_m is given by γ_m. We define the contact risk modifier between the susceptible human and the infectious mosquito as α, and the contact modifier for host-to-vector transmission as η. The biting rate of mosquitoes is given by b. The malaria-induced mortality rate in humans is denoted by δ.

The compartmental model is described by the following system of non-linear ordinary differential

equations:

$$\frac{dS_1}{dt} = \Lambda_h - \rho S_1 + \theta S_2 - \lambda_1 S_1 + (1-q)\sigma R_h + zkE_h - \mu_h S_1, \tag{1}$$
$$\frac{dS_2}{dt} = \rho S_1 - \theta S_2 - \lambda_2 S_2 + q\sigma R_h + (1-z)kE_h - \mu_h S_2, \tag{2}$$
$$\frac{dE_h}{dt} = \lambda_1 S_1 + \lambda_2 S_2 - (k + \gamma_h + \mu_h)E_h, \tag{3}$$
$$\frac{dA_h}{dt} = (1-\Phi)\gamma_h E_h - (\omega + \mu_h)A_h, \tag{4}$$
$$\frac{dI_h}{dt} = \Phi\gamma_h E_h + \chi\omega A_h - (\xi + \mu_h + \delta)I_h, \tag{5}$$
$$\frac{dT_h}{dt} = \xi I_h - (\alpha_1 + \mu_h + \tau)T_h, \tag{6}$$
$$\frac{dR_h}{dt} = \tau T_h + (1-\chi)\omega A_h - (\mu_h + \sigma)R_h, \tag{7}$$
$$\frac{dS_m}{dt} = \Lambda_m - \lambda_m S_m - \mu_m S_m, \tag{8}$$
$$\frac{dE_m}{dt} = \lambda_m S_m - (\gamma_m + \mu_m)E_m, \tag{9}$$
$$\frac{dI_m}{dt} = \gamma_m E_m - \mu_m I_m, \tag{10}$$

where the forces of infection for low-awareness humans (λ_1), high-awareness humans (λ_2), and mosquitoes (λ_m) are defined as:

$$\lambda_1 = \frac{\alpha\beta_h b I_m}{N_h}, \quad \lambda_2 = \frac{\alpha\beta_h b\alpha_3 I_m}{N_h}, \quad \lambda_m = \frac{\eta\beta_m b(A_h + \alpha_2 I_h)}{N_h}. \tag{11}$$

The total population sizes for humans (N_h) and vectors (N_m) are:

$$N_h = S_1 + S_2 + E_h + A_h + I_h + T_h + R_h, \tag{12}$$
$$N_m = S_m + E_m + I_m. \tag{13}$$

The initial conditions associated with the system (1)–(10) are:

$$\begin{aligned} &S_1(0) > 0, \quad S_2(0) > 0, \quad E_h(0) \geq 0, \quad A_h(0) \geq 0, \quad I_h(0) \geq 0, \\ &T_h(0) \geq 0, \quad R_h(0) \geq 0, \quad S_m(0) > 0, \quad E_m(0) \geq 0, \quad I_m(0) \geq 0. \end{aligned} \tag{14}$$

Table 1: State Variables Descriptions

Variable	Description
S_1	Susceptible population with high risk of malaria infection (low awareness level)
S_2	Susceptible population with low risk of malaria infection (high awareness level)
E_h	Exposed human population
A_h	Asymptomatic human population
I_h	Symptomatic human population
T_h	Treated human population
R_h	Recovered human population
S_m	Susceptible mosquito population
E_m	Exposed mosquito population
I_m	Infectious mosquito population

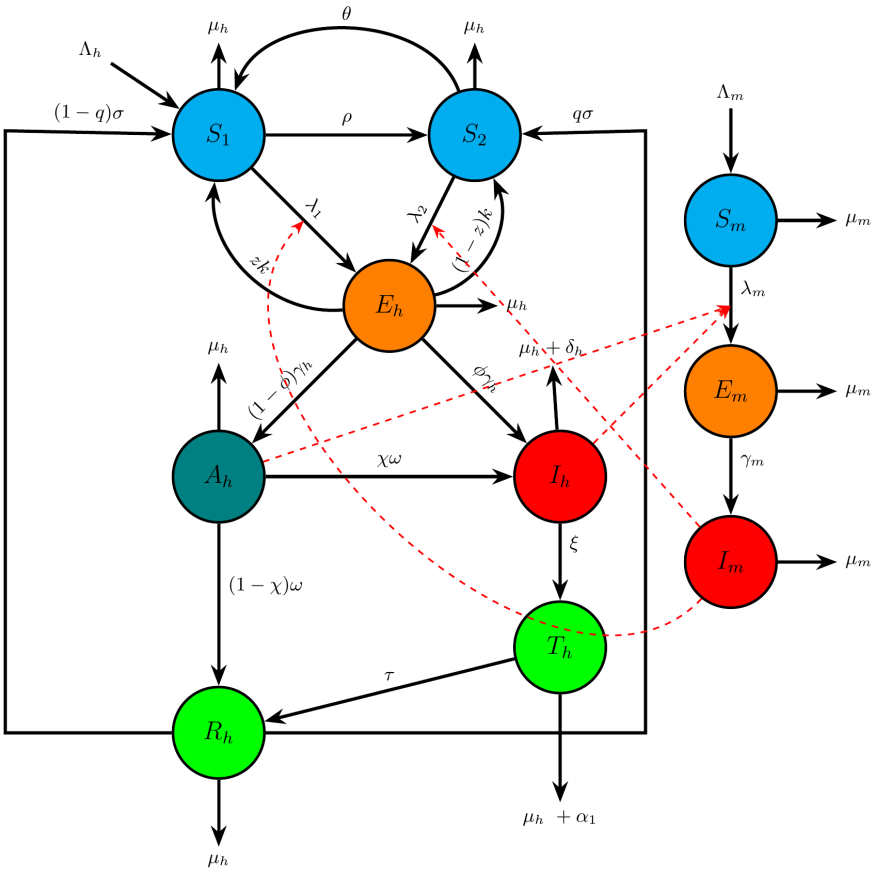

Figure 1: Flow diagram of the malaria transmission model illustrating transitions between human and vector compartments.

2.1 Assumptions of the model

- No age or spatial structure, i.e., all individuals within a compartment are identical.
- The time individuals spend in a compartment is exponentially distributed.
- Recovery confers complete but temporary immunity. Upon waning immunity, individuals become fully susceptible again with an equal chance of entering S_1 or S_2.
- The force of infection is uniform across the population. Every mosquito has an equal probability of biting any human, and every human has an equal probability of being bitten.
- Humans and mosquitoes cannot be infected by more than one strain of malaria simultaneously.
- Human risk is categorized into only two distinct groups, i.e., "high risk" and "low risk" or "low awareness level" and "high awareness level", respectively.
- The rate of bite prevention for the S_2 group is a constant value. It doesn't account for inconsistent bed net use, net quality variation, or insecticide resistance developing over time.
- Moving from S_1 to S_2 (i.e., receiving a bed net) instantly reduces an individual's risk. It doesn't account for the time it takes to adapt and consistently use the intervention.
- While mosquitoes' mortality can be increased, the model doesn't explicitly separate the effects of different vector control methods like IRS (Indoor Residual Spraying) and ITNs (Insecticide-Treated Nets), which may have a different impact on biting rates and mortality.

Table 2: Parameters Description

Parameter	Description
Λ_h	Human recruitment rate
Λ_m	Vector recruitment rate
θ	Rate at which S_2 returns to S_1 due to forgetfulness
ρ	Rate at which S_1 moves to S_2 (awareness program participation)
Φ	Fraction of infected individuals developing symptoms
ω	Progression rate from asymptomatic to symptomatic
γ_h	Rate at which exposed humans become infectious (progression rate)
ξ	Treatment rate of symptomatic humans
q	Fraction of treated humans returning to low-risk class after recovery
σ	Rate of loss of temporary immunity
α_3	Reduction in infection risk for S_2 due to LLIN use
γ_m	Rate at which exposed mosquitoes become infectious
α_2	Modification factor for infectiousness of symptomatic humans
α	Dimensionless contact/risk modification factor for human-mosquito contact
β_h	Transmission probability from infectious vector to human host
β_m	Transmission probability from infectious host to vector
b	Mosquito biting rate
η	Contact modifier for host-to-vector transmission
μ_h	Natural human mortality rate
μ_m	Natural mosquito mortality rate
δ	Malaria-induced mortality rate in humans
z	Fraction reverting from E_h to susceptible due to temporary immunity
k	Rate of immune recovery from exposed class
χ	Fraction progressing from asymptomatic to symptomatic class
α_1	Mortality rate due to treatment failure
τ	Recovery rate from treatment class

- Individuals in the population can die via natural mortality rate, which is not affected by malaria infection, by death due to treatment failure, or by death due to malaria infection.
- Mosquitoes have a natural lifespan, which is not affected by malaria infection.
- Asymptomatic individuals can recover due to their robust immune system.

3 Analysis of the Model

In this section, we provide a detailed mathematical and epidemiological analysis of the well-posedness of the malaria model. This includes proving the positivity and boundedness of solutions, establishing the existence of steady states, computing the basic reproduction number (R_0), and performing stability and sensitivity analyses. Detailed proofs and derivations are provided in Appendix A.

3.1 Existence and Uniqueness of Solution to the Model

Theorem 1: Consider the initial value problem associated with the malaria transmission model of equations (1)–(10) with initial conditions (11):

$$\frac{d\boldsymbol{X}}{dt} = F(\boldsymbol{X}), \qquad \boldsymbol{X}(0) = \boldsymbol{X}_0,$$

where $\boldsymbol{X}(t) = \big(S_1, S_2, E_h, A_h, I_h, T_h, R_h, S_m, E_m, I_m\big)^T \in \mathbb{R}^{10}$.

If the vector field $F : \mathbb{R}^{10} \to \mathbb{R}^{10}$ is continuous and locally Lipschitz on a domain $\Omega \subset \mathbb{R}^{10}$ that contains the initial point $\boldsymbol{X}_0$, then there exists a unique local solution $\boldsymbol{X}(t)$ defined on some interval $[0, T)$, $T > 0$.

Proof: We rewrite the equation (1)–(10) in vector form:

$$\frac{d\boldsymbol{X}}{dt} = F(\boldsymbol{X}),$$

where each component $F_i(\boldsymbol{X})$ consists of polynomial and rational expressions involving the state variables and parameters (see Section 2 of the paper).

Every component of $F(\boldsymbol{X})$ is built from addition, multiplication, and division by the positive quantity

$$N_h = S_1 + S_2 + E_h + A_h + I_h + T_h + R_h.$$

Over the biologically feasible region,

$$\Omega \subset \mathbb{R}^{10}_{+} : N_h > 0,\ N_m > 0,$$

all such operations are continuous. Hence, F is continuous on Ω. This satisfies the first hypothesis of the Picard–Lindelöf Theorem.

To establish local Lipschitz continuity, it suffices to show that the Jacobian matrix,

$$J(\boldsymbol{X}) = \frac{\partial F}{\partial \boldsymbol{X}},$$

exists and is continuous on Ω.

From the structure of the system, each $F_i(\boldsymbol{X})$ is linear or bilinear in the state variables; all partial derivatives $\frac{\partial F_i}{\partial X_j}$ are therefore polynomials or rational functions with a denominator N_h, and since $N_h > 0$ in the domain Ω, each component of $J(\boldsymbol{X})$ is continuous. Because the Jacobian is continuous on any compact subset $K \subset \Omega$, it is bounded there. Thus,

$$\|F(\boldsymbol{X}) - F(\boldsymbol{Y})\| \leq L\|\boldsymbol{X} - \boldsymbol{Y}\| \quad \forall\, \boldsymbol{X}, \boldsymbol{Y} \in K$$

for some constant $L > 0$. Hence, F is locally Lipschitz on Ω. This verifies the second hypothesis of the theorem.

Since F is continuous and locally Lipschitz in $\boldsymbol{X}$, the Picard–Lindelöf theorem guarantees:

- existence of a solution $\boldsymbol{X}(t)$ on a neighborhood of $t = 0$,
- uniqueness of this solution in that neighborhood,
- continuous dependence on the initial conditions.

Thus, for all biologically feasible initial values

$$\boldsymbol{X}_0 = \big(S_1(0), S_2(0), E_h(0), A_h(0), I_h(0), T_h(0), R_h(0), S_m(0), E_m(0), I_m(0)\big),$$

there exists a unique local solution to the malaria model.

3.2 Positivity and Boundedness of the Malaria Model

3.2.1 Positivity of the Model

Theorem 2: Every solution of the model equations (1)–(10) with non-negative initial conditions in $\mathbb{R}^{10}_{+}$ remains non-negative for all $t > 0$. Specifically, if the initial conditions satisfy $S_1(0) \geq 0$, $S_2(0) \geq 0$, $E_h(0) \geq 0$, $A_h(0) \geq 0$, $I_h(0) \geq 0$, $T_h(0) \geq 0$, $R_h(0) \geq 0$, $S_m(0) \geq 0$, $E_m(0) \geq 0$, and $I_m(0) \geq 0$,

then the solution trajectory $(S_1(t), S_2(t), E_h(t), A_h(t), I_h(t), T_h(t), R_h(t), S_m(t), E_m(t), I_m(t))$ remains in the non-negative orthant $\mathbb{R}^{10}_+$ for all $t \geq 0$.

Proof: Considering each of the differential equations separately,

From the first equation in the set:

$$\frac{dS_1}{dt} = \Lambda_h - \rho S_1 + \theta S_2 - \lambda_1 S_1 + (1-q)\sigma R_h + zkE_h - \mu_h S_1.$$

Since Λ_h, θS_2, $(1-q)\sigma R_h$, and zkE_h are positive, we drop them, such that the equation above can be written as:

$$\frac{dS_1}{dt} \geq -(\rho + \lambda_1 + \mu_h)S_1.$$

By separation of variables and integrating both sides of the equation above, we have

$$S_1 \geq ke^{-(\rho+\lambda_1+\mu_h)t}.$$

Applying the initial condition, $S_1(0) \geq 0$, we get:

$$S_1(t) \geq S_1(0)e^{-(\rho+\lambda_1+\mu_h)t} \geq 0,$$

since the initial population size of susceptible with high risk is positive, i.e. $S_1(0) \geq 0$, and the exponential function is always non-negative. It can be concluded that $S_1(t)$ is positive.

Also, taking the third equation:

$$\frac{dE_h}{dt} = \lambda_1 S_1 + \lambda_2 S_2 - (k + \gamma_h + \mu_h)E_h.$$

The equation reduces to:

$$\frac{dE_h}{dt} \geq -(k + \gamma_h + \mu_h)E_h.$$

By separation of variables and integrating both sides of the equation above, we have

$$E_h \geq Ae^{-(k+\gamma_h+\mu_h)t}.$$

Applying the initial condition, $E_h(0) \geq 0$, we have:

$$E_h(t) \geq E_h(0)e^{-(k+\gamma_h+\mu_h)t}.$$

Since the initial population size of exposed is positive, i.e. $E_h(0) \geq 0$, and the exponential function is always non-negative, it can be concluded that $E_h(t)$ is positive.

Similarly, the same integration procedure can be applied to the remaining compartments, ensuring that all state variables remain non-negative for all $t \geq 0$.

3.2.2 Boundedness of the Model

Summing up all of the human compartments and the mosquito compartments gives,

$$N_h = S_1 + S_2 + E_h + A_h + I_h + T_h + R_h, \tag{12}$$

$$N_m = S_m + E_m + I_m. \tag{13}$$

Taking the derivative across (12) for all compartments, we get:

$$\frac{dN_h}{dt} = \frac{dS_1}{dt} + \frac{dS_2}{dt} + \frac{dE_h}{dt} + \frac{dA_h}{dt} + \frac{dI_h}{dt} + \frac{dT_h}{dt} + \frac{dR_h}{dt}.$$

Reverting to the first seven equations of the malaria model, this reduces to:

$$\frac{dN_h}{dt} = \Lambda_h - \mu_h N_h - \delta I_h - \alpha_1 T_h.$$

Thus,

$$\frac{dN_h}{dt} \leq \Lambda_h - \mu_h N_h,$$
$$\frac{dN_h}{dt} + \mu_h N_h \leq \Lambda_h. \tag{14}$$

Solving (14) using the integrating factor method, this gives:

$$N_h(t) \leq \frac{\Lambda_h}{\mu_h} + Ce^{-\mu_h t}. \tag{15}$$

Notice that from (15), when $t = 0$, we get:

$$C = N_h(0) - \frac{\Lambda_h}{\mu_h}.$$

Then, (15) becomes:

$$N_h(t) \leq \frac{\Lambda_h}{\mu_h} + \left(N_h(0) - \frac{\Lambda_h}{\mu_h}\right) e^{-\mu_h t}.$$

As $t \to \infty$, $e^{-\mu_h t} \to 0$, therefore,

$$0 < N_h \leq \frac{\Lambda_h}{\mu_h}.$$

Thus, we have the human population as:

$$N_h \leq \frac{\Lambda_h}{\mu_h}.$$

Hence,

$$\pi_h = \left\{(S_1, S_2, E_h, A_h, I_h, T_h, R_h) \in \mathbb{R}^7_+ : S_1(0) > 0,\ S_2(0), E_h(0), A_h(0), I_h(0), T_h(0), R_h(0) \geq 0,\ N_h \leq \frac{\Lambda_h}{\mu_h}\right\}.$$

Similarly, for the mosquito population, we have,

$$\pi_v = \left\{(S_m, E_m, I_m) \in \mathbb{R}^3_+, \quad S_m(0) > 0, E_m(0) \geq 0, I_m(0) \geq 0, \quad N_m \leq \frac{\Lambda_m}{\mu_m}\right\}.$$

3.3 The Malaria-Free Equilibrium Point and The Reproduction Number

3.3.1 The Malaria-Free Equilibrium Point

The malaria-free equilibrium point (MFEP), E_0, represents the steady state of the system in the absence of infection. To determine E_0, we set all infected compartments to zero ($E_h = A_h = I_h = T_h = R_h = E_m = I_m = 0$), equate the remaining derivatives to zero, and solve the algebraic system. This yields:

$$E_0 = \left(S_1^*, S_2^*, E_h^*, A_h^*, I_h^*, T_h^*, R_h^*, S_m^*, E_m^*, I_m^*\right) = \left(\frac{\Lambda_h(\theta + \mu_h)}{\mu_h(\rho + \theta + \mu_h)},\ \frac{\rho\Lambda_h}{\mu_h(\rho + \theta + \mu_h)},\ 0,\ 0,\ 0,\ 0,\ 0,\ \frac{\Lambda_m}{\mu_m},\ 0,\ 0\right).$$

3.3.2 The Reproduction Number

The basic reproduction number, denoted as R_0, represents the expected number of secondary cases generated by a single infectious individual introduced into a completely susceptible population [13]. If $R_0 > 1$, the disease can invade and persist; if $R_0 < 1$, the disease dies out.

To compute the basic reproduction number R_0, we apply the next-generation matrix method formulated by Van den Driessche and Watmough [14]. We partition the state variables associated with infected compartments into the vector:

$$\boldsymbol{X} = (E_h,\ A_h,\ I_h,\ T_h,\ R_h,\ E_m,\ I_m)^T.$$

The rate of appearance of new infections in these compartments is represented by the transmission vector $\mathcal{F}$, while the rate of transfer of individuals out of or between these compartments is represented by the transition vector $\mathcal{V}$. From the system (1)–(10) evaluated at the disease-free equilibrium (DFE), E_0, we obtain:

$$\mathcal{F} = \begin{pmatrix} \frac{\alpha\beta_h b(\alpha_3\rho+\theta+\mu_h)I_m}{\rho+\theta+\mu_h} \\ 0 \\ 0 \\ 0 \\ 0 \\ \frac{\eta\beta_m b\Lambda_m\mu_h(A_h+\alpha_2 I_h)}{\Lambda_h\mu_m} \\ 0 \end{pmatrix}, \qquad \mathcal{V} = \begin{pmatrix} (k+\gamma_h+\mu_h)E_h \\ -(1-\Phi)\gamma_h E_h + (\omega+\mu_h)A_h \\ -\Phi\gamma_h E_h - \chi\omega A_h + (\xi+\mu_h+\delta)I_h \\ -\xi I_h + (\alpha_1+\tau+\mu_h)T_h \\ -\tau T_h - (1-\chi)\omega A_h + (\mu_h+\sigma)R_h \\ (\gamma_m+\mu_m)E_m \\ -\gamma_m E_m + \mu_m I_m \end{pmatrix}.$$

The corresponding Jacobian matrices of $\mathcal{F}$ and $\mathcal{V}$ evaluated at E_0 are, respectively:

$$F = \begin{pmatrix} 0 & 0 & 0 & 0 & 0 & 0 & \frac{\alpha\beta_h b(\alpha_3\rho+\theta+\mu_h)}{\rho+\theta+\mu_h} \\ 0 & 0 & 0 & 0 & 0 & 0 & 0 \\ 0 & 0 & 0 & 0 & 0 & 0 & 0 \\ 0 & 0 & 0 & 0 & 0 & 0 & 0 \\ 0 & 0 & 0 & 0 & 0 & 0 & 0 \\ 0 & \frac{\eta\beta_m b\Lambda_m\mu_h}{\Lambda_h\mu_m} & \frac{\eta\beta_m b\Lambda_m\mu_h\alpha_2}{\Lambda_h\mu_m} & 0 & 0 & 0 & 0 \\ 0 & 0 & 0 & 0 & 0 & 0 & 0 \end{pmatrix},$$

and

$$V = \begin{pmatrix} k+\gamma_h+\mu_h & 0 & 0 & 0 & 0 & 0 & 0 \\ -(1-\Phi)\gamma_h & \omega+\mu_h & 0 & 0 & 0 & 0 & 0 \\ -\Phi\gamma_h & -\chi\omega & \xi+\mu_h+\delta & 0 & 0 & 0 & 0 \\ 0 & 0 & -\xi & \alpha_1+\tau+\mu_h & 0 & 0 & 0 \\ 0 & -(1-\chi)\omega & 0 & -\tau & \mu_h+\sigma & 0 & 0 \\ 0 & 0 & 0 & 0 & 0 & \gamma_m+\mu_m & 0 \\ 0 & 0 & 0 & 0 & 0 & -\gamma_m & \mu_m \end{pmatrix}.$$

The next-generation matrix is defined as $K = FV^{-1}$. To do this, we first compute the overall transition inverse matrix V^{-1}:

$$V^{-1} = \begin{pmatrix} \frac{1}{v_1} & 0 & 0 & 0 & 0 & 0 & 0 \\ \frac{(1-\Phi)\gamma_h}{v_1 v_2} & \frac{1}{v_2} & 0 & 0 & 0 & 0 & 0 \\ \frac{\gamma_h[\Phi v_2+\chi\omega(1-\Phi)]}{v_1 v_2 v_3} & \frac{\chi\omega}{v_2 v_3} & \frac{1}{v_3} & 0 & 0 & 0 & 0 \\ \frac{\xi\gamma_h[\Phi v_2+\chi\omega(1-\Phi)]}{v_1 v_2 v_3 v_4} & \frac{\xi\chi\omega}{v_2 v_3 v_4} & \frac{\xi}{v_3 v_4} & \frac{1}{v_4} & 0 & 0 & 0 \\ (V^{-1})_{5,1} & \frac{(1-\chi)\omega v_3 v_4+\tau\xi\chi\omega}{v_2 v_3 v_4 v_5} & \frac{\tau\xi}{v_3 v_4 v_5} & \frac{\tau}{v_4 v_5} & \frac{1}{v_5} & 0 & 0 \\ 0 & 0 & 0 & 0 & 0 & \frac{1}{v_6} & 0 \\ 0 & 0 & 0 & 0 & 0 & \frac{\gamma_m}{\mu_m v_6} & \frac{1}{\mu_m} \end{pmatrix},$$

where the entry $(V^{-1})_{5,1}$ is:

$$(V^{-1})_{5,1} = \frac{(1-\chi)\omega(1-\Phi)\gamma_h v_3 v_4 + \tau\xi\gamma_h[\Phi v_2 + \chi\omega(1-\Phi)]}{v_1 v_2 v_3 v_4 v_5},$$

and the intermediate variables $v_1, \ldots, v_6$ are defined in Section 3.4.

Multiplying the transmission Jacobian matrix F by V^{-1} yields the next-generation matrix $K = FV^{-1}$:

$$K = \begin{pmatrix} 0 & 0 & 0 & 0 & 0 & K_{1,6} & K_{1,7} \\ 0 & 0 & 0 & 0 & 0 & 0 & 0 \\ 0 & 0 & 0 & 0 & 0 & 0 & 0 \\ 0 & 0 & 0 & 0 & 0 & 0 & 0 \\ 0 & 0 & 0 & 0 & 0 & 0 & 0 \\ K_{6,1} & K_{6,2} & K_{6,3} & 0 & 0 & 0 & 0 \\ 0 & 0 & 0 & 0 & 0 & 0 & 0 \end{pmatrix},$$

where the non-zero entries are:

$$\begin{aligned}
K_{1,6} &= \frac{\alpha\beta_h b\gamma_m(\alpha_3\rho + \theta + \mu_h)}{\mu_m v_6(\rho + \theta + \mu_h)}, \\
K_{1,7} &= \frac{\alpha\beta_h b(\alpha_3\rho + \theta + \mu_h)}{\mu_m(\rho + \theta + \mu_h)}, \\
K_{6,1} &= \frac{\eta\beta_m b\Lambda_m\mu_h\gamma_h[(1-\Phi)v_3 + \alpha_2\Phi v_2 + \alpha_2\chi\omega(1-\Phi)]}{\Lambda_h\mu_m v_1 v_2 v_3}, \\
K_{6,2} &= \frac{\eta\beta_m b\Lambda_m\mu_h[v_3 + \alpha_2\chi\omega]}{\Lambda_h\mu_m v_2 v_3}, \\
K_{6,3} &= \frac{\eta\beta_m b\Lambda_m\mu_h\alpha_2}{\Lambda_h\mu_m v_3}.
\end{aligned}$$

Evaluating to obtain the eigenvalues of the matrix K above and further specifying the largest dominant eigenvalue of the matrix K (spectral radius $\rho(K)$), we obtain the explicit mathematical expression for the basic reproduction number:

$$R_0 = \sqrt{\frac{b^2\beta_h\beta_m\Lambda_m\alpha\eta\gamma_h\gamma_m\mu_h(\alpha_3\rho + \mu_h + \theta)\left[\alpha_2\Phi(\mu_h+\omega) + (1-\Phi)(\alpha_2\chi\omega + \mu_h + \xi + \delta)\right]}{\mu_m^2\Lambda_h(\gamma_m+\mu_m)(\mu_h+\omega)(k+\gamma_h+\mu_h)(\delta+\xi+\mu_h)(\rho+\theta+\mu_h)}}.$$

3.3.3 Biological Interpretation and Decomposition of the Reproduction Number

To understand the transmission mechanisms of malaria in the model, the basic reproduction number R_0 can be decomposed into the contributions of the asymptomatic (A_h) and symptomatic (I_h) classes:

$$R_0 = \sqrt{R_{0A}^2 + R_{0I}^2},$$

where R_{0A} represents the reproduction number of the transmission loop via the asymptomatic class (A_h), and R_{0I} represents the reproduction number of the transmission loop via the symptomatic class (I_h). These components are expressed analytically as:

$$\begin{aligned}
R_{0A} &= \sqrt{C_0 \cdot \frac{1-\Phi}{\omega + \mu_h}}, \\
R_{0I} &= \sqrt{C_0 \cdot \alpha_2\left[\frac{\Phi}{\delta+\xi+\mu_h} + \frac{\chi\omega(1-\Phi)}{(\omega+\mu_h)(\delta+\xi+\mu_h)}\right]},
\end{aligned}$$

where C_0 is the baseline transmission multiplier defined by:

$$C_0 = \frac{b^2\alpha\beta_h\beta_m\Lambda_m\eta\gamma_h\gamma_m\mu_h(\alpha_3\rho+\mu_h+\theta)}{\mu_m^2\Lambda_h(\gamma_m+\mu_m)(k+\gamma_h+\mu_h)(\rho+\theta+\mu_h)}.$$

Alternatively, the square of the basic reproduction number, R_0^2, can be interpreted as the product of two distinct transmission pathways:

$$R_0^2 = T_{m\to h} \times T_{h\to m},$$

where $T_{m\to h}$ represents the average number of humans infected by a single infectious mosquito over its lifespan, and $T_{h\to m}$ represents the average number of mosquitoes infected by a single infectious human over their infectious period.

Mosquito-to-Human Transmission ($T_{m\to h}$): The factor representing transmission from vectors to hosts is given by:

$$T_{m\to h} = [b\cdot(\alpha\beta_h)]\cdot\left[\frac{\gamma_m}{\gamma_m+\mu_m}\right]\cdot\left[\frac{1}{\mu_m}\right]\cdot\left[\frac{\alpha_3\rho+\theta+\mu_h}{\rho+\theta+\mu_h}\right],$$

where each term has the following biological meaning:

- $b\cdot(\alpha\beta_h)$: The transmission rate per mosquito per bite. Here, b is the biting rate, β_h is the transmission probability from mosquito to human, and α is the contact modifier.
- $\frac{\gamma_m}{\gamma_m+\mu_m}$: The probability that an exposed mosquito survives the latency (incubation) period to become infectious, where γ_m is the progression rate and μ_m is the vector mortality rate.
- $\frac{1}{\mu_m}$: The average lifespan of a mosquito.
- $\frac{\alpha_3\rho+\theta+\mu_h}{\rho+\theta+\mu_h}$: The average susceptibility of the human population at the DFE. This is the sum of the proportion of high-risk susceptibles ($\frac{\theta+\mu_h}{\rho+\theta+\mu_h}$) and the proportion of low-risk susceptibles ($\frac{\rho}{\rho+\theta+\mu_h}$) weighted by their respective risk modification factors (1 and α_3).

Human-to-Mosquito Transmission ($T_{h\to m}$): The factor representing transmission from hosts to vectors is given by:

$$T_{h\to m} = \left[b\cdot\frac{N_m^*}{N_h^*}\cdot(\eta\beta_m)\right]\cdot\left[\frac{\gamma_h}{k+\gamma_h+\mu_h}\right]\cdot\left[\frac{1-\Phi}{\omega+\mu_h}+\frac{\alpha_2\Phi}{\xi+\mu_h+\delta}+\frac{\alpha_2\chi\omega(1-\Phi)}{(\omega+\mu_h)(\xi+\mu_h+\delta)}\right],$$

where $N_h^* = \frac{\Lambda_h}{\mu_h}$ and $N_m^* = \frac{\Lambda_m}{\mu_m}$ are the DFE population sizes, and each term represents:

- $b\cdot\frac{N_m^*}{N_h^*}\cdot(\eta\beta_m)$: The transmission rate per human host. This is the product of the mosquito biting rate on humans ($b\frac{N_m^*}{N_h^*}$) and the transmission probability from host to vector ($\eta\beta_m$).
- $\frac{\gamma_h}{k+\gamma_h+\mu_h}$: The probability that an exposed human survives the latent period to become infectious, where γ_h is the human progression rate.
- The final sum represents the average infectious duration of an infected human:
  - $\frac{1-\Phi}{\omega+\mu_h}$: The average time an infected human spends in the asymptomatic compartment (A_h), where $1-\Phi$ is the probability of becoming asymptomatic.
  - $\frac{\alpha_2\Phi}{\xi+\mu_h+\delta}$: The average time an infected human spends in the symptomatic compartment (I_h) if they develop symptoms directly (probability Φ), weighted by their relative infectiousness modifier α_2.

- $\frac{\alpha_2\chi\omega(1-\Phi)}{(\omega+\mu_h)(\xi+\mu_h+\delta)}$: The average time individuals spend in the symptomatic compartment (I_h) if they transition from the asymptomatic state (probability $\frac{\chi\omega(1-\Phi)}{\omega+\mu_h}$), weighted by α_2.

Biological Interpretation and Dimensional Consistency of the Asymptomatic Factor: The term $(1-\Phi)(\alpha_2\chi\omega+\mu_h+\xi+\delta)$ in the asymptomatic contribution to R_0 represents the total transmission potential initiated by individuals who enter the asymptomatic state (A_h).

Mathematically, when we combine the direct asymptomatic transmission and the indirect symptomatic transmission (from asymptomatic carriers who clinically progress to the symptomatic compartment), the sum of these two paths is:

$$\frac{1-\Phi}{\omega+\mu_h}+\frac{\alpha_2\chi\omega(1-\Phi)}{(\omega+\mu_h)(\xi+\mu_h+\delta)}=\frac{1-\Phi}{(\omega+\mu_h)(\xi+\mu_h+\delta)}\left[\alpha_2\chi\omega+\mu_h+\xi+\delta\right].$$

Here, the multiplier $\frac{1-\Phi}{(\omega+\mu_h)(\xi+\mu_h+\delta)}$ represents the probability of entering the asymptomatic stage scaled by the durations of both stages. The term inside the brackets, $(\alpha_2\chi\omega+\mu_h+\xi+\delta)$, is the sum of the direct exit rates from the symptomatic compartment (natural mortality μ_h, treatment rate ξ, and disease-induced death rate δ) and the progression rate from asymptomatic to symptomatic state scaled by the relative infectiousness α_2.

This expression is dimensionally consistent, as every term within the parentheses has the unit of time^{-1} (or day^{-1}): μ_h, ξ, and δ are transition rates, and the product of the dimensionless parameters α_2 and χ with the progression rate ω yields a rate in day^{-1}.

Remark on Numerical Evaluation and Transient Dynamics: Using the baseline parameter values from Table 4, the uninfected disease-free equilibrium (DFE) total population sizes are $N_h^*=\frac{\Lambda_h}{\mu_h}\approx 2.201\times10^6$ for humans and $N_m^*=\frac{\Lambda_m}{\mu_m}\approx 4.5\times10^5$ for mosquitoes. Substituting these equilibrium values into the derived formula yields a theoretical basic reproduction number of $R_0\approx 0.345<1$, which indicates that the disease-free equilibrium is locally stable and the disease will eventually die out in the long run.

However, in the numerical simulations (Section 4), the system is initialized in a localized community where the human population is $N_h(0)=8433$ and the vector population is $N_m(0)=950$ (from Table 3). During the transient phase (e.g., $t\in[0,200]$ days), the mosquito population grows rapidly towards its carrying capacity while the human population grows much more slowly. At $t=25$ days, the vector-to-host ratio reaches 6.63 mosquitoes per human, which is nearly 35 times larger than the ratio at the DFE (approximately 0.20). Consequently, the effective reproduction number during this transient window is $R_0^{\text{eff}}(t)=R_0\sqrt{\frac{N_m(t)}{N_h(t)}\frac{N_h^*}{N_m^*}}=0.3447\times\sqrt{\frac{6.63}{0.2045}}=0.3447\times\sqrt{32.42}=0.3447\times5.69\approx\mathbf{1.96}$, causing the infection to grow and persist. Long-term simulations confirm that the disease eventually reaches a stable endemic state of $N_h\approx80,993$ due to the feedback of disease-induced mortality, and only dies out if $N_h(t)$ is artificially maintained near N_h^*.

3.4. Local Stability of the Malaria-Free Equilibrium Point

Theorem 3: The MFEP E_0 of equations (1)–(10) is locally asymptotically stable if $R_0<1$ and unstable if $R_0>1$.

Proof: This is determined by first evaluating the Jacobian matrix $J(E_0)$ of equations (1)–(10) at MFEP E_0, which is given as:

$$J(E_0) = \begin{pmatrix} -(\rho+\mu_h) & \theta & zk & 0 & 0 & 0 & 0 & 0 & 0 & -a_1 \\ \rho & -(\theta+\mu_h) & (1-z)k & 0 & 0 & 0 & 0 & 0 & 0 & -a_2 \\ 0 & 0 & -v_1 & 0 & 0 & 0 & 0 & 0 & 0 & a_1+a_2 \\ 0 & 0 & (1-\Phi)\gamma_h & -v_2 & 0 & 0 & 0 & 0 & 0 & 0 \\ 0 & 0 & \Phi\gamma_h & \chi\omega & -v_3 & 0 & 0 & 0 & 0 & 0 \\ 0 & 0 & 0 & 0 & \xi & -v_4 & 0 & 0 & 0 & 0 \\ 0 & 0 & 0 & (1-\chi)\omega & 0 & \tau & -v_5 & 0 & 0 & 0 \\ 0 & 0 & 0 & -b_1 & -b_2 & 0 & 0 & -\mu_m & 0 & 0 \\ 0 & 0 & 0 & b_1 & b_2 & 0 & 0 & 0 & -v_6 & 0 \\ 0 & 0 & 0 & 0 & 0 & 0 & 0 & 0 & \gamma_m & -\mu_m \end{pmatrix},$$

where:

$$a_1 = \frac{\alpha\beta_h b S_1^*}{N_h^*}, \quad a_2 = \frac{\alpha\beta_h b\alpha_3 S_2^*}{N_h^*}, \quad b_1 = \frac{\eta\beta_m b S_m^*}{N_h^*}, \quad b_2 = \frac{\eta\beta_m b\alpha_2 S_m^*}{N_h^*},$$
$$v_1 = k+\gamma_h+\mu_h, \quad v_2 = \omega+\mu_h, \quad v_3 = \xi+\mu_h+\delta, \quad v_4 = \alpha_1+\mu_h+\tau, \quad v_5 = \sigma+\mu_h, \quad v_6 = \gamma_m+\mu_m,$$

and S_1^*, S_2^*, and S_m^* are given respectively in Section 3.3.1.

The characteristic equation of the matrix J is given by $|J(E_0) - \lambda I| = 0$, where λ represents the eigenvalues of the matrix, and I is the identity matrix. For the given 10×10 Jacobian matrix, a direct expansion of the determinant is computationally intensive. However, the matrix has a specific block structure that allows for significant simplification.

By reordering the state variables, the matrix can be shown to be block lower triangular. The characteristic polynomial of a block triangular matrix is the product of the characteristic polynomials of its diagonal blocks. The eigenvalues of the entire matrix are the collection of the eigenvalues of these diagonal blocks.

The state variables can be partitioned into three epidemiologically significant groups that reveal this block structure:

- Human Susceptible-Exposed Subsystem: $\{S_1, S_2, E_h\}$,
- Infected/Recovered Human Subsystem: $\{A_h, I_h, T_h, R_h\}$,
- Vector (Mosquito) Subsystem: $\{S_m, E_m, I_m\}$.

The characteristic polynomial $P(\lambda)$ of the full Jacobian matrix is the product of the characteristic polynomials of the submatrices corresponding to these groups:

$$P(\lambda) = P_1(\lambda) \cdot P_2(\lambda) \cdot P_3(\lambda) = 0.$$

The characteristic polynomial for each block is derived as thus:**Infected/Recovered Human Subsystem:** $P_1(\lambda)$
The submatrix for the states $\{A_h, I_h, T_h, R_h\}$ (rows and columns 4, 5, 6, 7) is:

$$J_1 = \begin{pmatrix} -v_2 & 0 & 0 & 0 \\ \chi\omega & -v_3 & 0 & 0 \\ 0 & \xi & -v_4 & 0 \\ (1-\chi)\omega & 0 & \tau & -v_5 \end{pmatrix}.$$

This is a lower triangular matrix. The characteristic polynomial of a triangular matrix is the product of the terms on its diagonal:

$$\det(J_1 - \lambda I) = (-v_2-\lambda)(-v_3-\lambda)(-v_4-\lambda)(-v_5-\lambda).$$

Thus, the first part of the characteristic polynomial is:

$$P_1(\lambda) = (\lambda + v_2)(\lambda + v_3)(\lambda + v_4)(\lambda + v_5).$$

This gives four eigenvalues directly: $\lambda = -v_2,\ -v_3,\ -v_4,\ -v_5$.
Vector Subsystem: $P_2(\lambda)$
The submatrix for the vector states $\{S_m, E_m, I_m\}$ (rows and columns 8, 9, 10) is:

$$J_2 = \begin{pmatrix} -\mu_m & 0 & 0 \\ 0 & -v_6 & 0 \\ 0 & \gamma_m & -\mu_m \end{pmatrix}.$$

The characteristic polynomial for this block is:

$$\det(J_2 - \lambda I) = (-\mu_m - \lambda)(-v_6 - \lambda)(-\mu_m - \lambda).$$

Thus, the second part of the characteristic polynomial is:

$$P_2(\lambda) = (\lambda + \mu_m)^2(\lambda + v_6).$$

This gives three eigenvalues: $\lambda = -\mu_m$ (with multiplicity 2) and $\lambda = -v_6$.
Human Susceptible-Exposed Subsystem: $P_3(\lambda)$
The remaining block corresponds to the states $\{S_1, S_2, E_h\}$. The submatrix is:

$$J_3 = \begin{pmatrix} -\rho - \mu_h & \theta & zk \\ \rho & -\theta - \mu_h & (1-z)k \\ 0 & 0 & -v_1 \end{pmatrix}.$$

The characteristic equation for this block is $\det(J_3 - \lambda I) = 0$: Expanding the determinant along the third row gives:

$$\begin{aligned} P_3(\lambda) &= (-v_1 - \lambda) \cdot [(-\rho - \mu_h - \lambda)(-\theta - \mu_h - \lambda) - \rho\theta] \\ &= -(\lambda + v_1) \cdot [(\lambda + \rho + \mu_h)(\lambda + \theta + \mu_h) - \rho\theta] \\ &= -(\lambda + v_1) \cdot \left[\lambda^2 + (\rho + \theta + 2\mu_h)\lambda + (\rho + \mu_h)(\theta + \mu_h) - \rho\theta\right] \\ &= -(\lambda + v_1) \cdot \left[\lambda^2 + (\rho + \theta + 2\mu_h)\lambda + \mu_h^2 + \mu_h(\rho + \theta)\right]. \end{aligned}$$

Combining these parts, the full characteristic equation $\det(J(E_0) - \lambda I) = 0$ is given by the polynomial:

$$P(\lambda) = -(\lambda+v_1)(\lambda+v_2)(\lambda+v_3)(\lambda+v_4)(\lambda+v_5)(\lambda+v_6)(\lambda+\mu_m)^2\left[\lambda^2 + (\rho + \theta + 2\mu_h)\lambda + \mu_h(\mu_h + \rho + \theta)\right] = 0.$$

The polynomial $P(\lambda)$ is of degree 10. The roots (eigenvalues) of the polynomial are:

$$\begin{aligned} &\lambda_1 = -v_2, \quad \lambda_2 = -v_3, \quad \lambda_3 = -v_4, \quad \lambda_4 = -v_5, \quad \lambda_5 = -v_6, \\ &\lambda_{6,7} = -\mu_m, \quad \lambda_8 = -v_1, \end{aligned}$$

and λ_9, λ_{10} are the roots of the quadratic equation

$$\lambda^2 + (\rho + \theta + 2\mu_h)\lambda + \mu_h(\mu_h + \rho + \theta) = 0. \tag{15}$$

The provided values for v_1 through v_6 are:

$$v_1 = k+\gamma_h+\mu_h, \quad v_2 = \omega+\mu_h, \quad v_3 = \xi+\mu_h+\delta, \quad v_4 = \alpha_1+\mu_h+\tau, \quad v_5 = \sigma+\mu_h, \quad v_6 = \gamma_m+\mu_m.$$

We can see that all eigenvalues of the Jacobian are either negative or have negative real parts (since the quadratic equation (15) has positive coefficients, implying roots with negative real parts by the Routh–Hurwitz criterion). Hence, the DFE given in Section 3.3.1 is locally asymptotically stable.

3.5. Global Stability of the Malaria-Free Equilibrium Point

In this subsection, we establish the global stability of the DFE using a linear Lyapunov function.

Theorem 3.1. *The Disease-Free Equilibrium E_0 of the system (1)–(10) is globally asymptotically stable (G.A.S.) in the region Ω if $R_0 < 1$.*

Proof. Consider the following linear Lyapunov function:

$$L = w_1 E_h + w_2 A_h + w_3 I_h + w_4 E_m + w_5 I_m, \tag{16}$$

where w_1, w_2, w_3, w_4, w_5 are positive constants to be determined. The time derivative of L along the trajectories of the system is given by:

$$\frac{dL}{dt} = w_1 \frac{dE_h}{dt} + w_2 \frac{dA_h}{dt} + w_3 \frac{dI_h}{dt} + w_4 \frac{dE_m}{dt} + w_5 \frac{dI_m}{dt}. \tag{17}$$

Substituting the rate equations (3), (4), (5), (9), and (10):

$$\begin{aligned} \frac{dL}{dt} =& w_1 \left[\frac{\alpha \beta_h b (S_1 + \alpha_3 S_2) I_m}{N_h} - v_1 E_h \right] \\ &+ w_2 \left[(1-\Phi)\gamma_h E_h - v_2 A_h \right] \\ &+ w_3 \left[\Phi \gamma_h E_h + \chi \omega A_h - v_3 I_h \right] \\ &+ w_4 \left[\frac{\eta \beta_m b (A_h + \alpha_2 I_h) S_m}{N_h} - v_6 E_m \right] \\ &+ w_5 \left[\gamma_m E_m - \mu_m I_m \right]. \end{aligned} \tag{18}$$

Grouping terms by the infected state variables yields:

$$\begin{aligned} \frac{dL}{dt} =& \left[-w_1 v_1 + w_2 (1-\Phi)\gamma_h + w_3 \Phi \gamma_h \right] E_h \\ &+ \left[-w_2 v_2 + w_3 \chi \omega + w_4 \frac{\eta \beta_m b S_m}{N_h} \right] A_h \\ &+ \left[-w_3 v_3 + w_4 \frac{\eta \beta_m b \alpha_2 S_m}{N_h} \right] I_h \\ &+ \left[-w_4 v_6 + w_5 \gamma_m \right] E_m \\ &+ \left[w_1 \frac{\alpha \beta_h b (S_1 + \alpha_3 S_2)}{N_h} - w_5 \mu_m \right] I_m. \end{aligned} \tag{19}$$

Since the susceptible populations are bounded in the invariant region Ω, we can write:

$$S_1 \leq S_1^*, \quad S_2 \leq S_2^*, \quad S_m \leq S_m^*, \quad N_h \geq S_1 + S_2. \tag{20}$$

We establish upper bounds for the coefficients of the disease states by setting:

$$w_4 v_6 = w_5 \gamma_m \implies w_4 = w_5 \frac{\gamma_m}{v_6}, \tag{21}$$

$$w_3 v_3 = w_4 \frac{\eta \beta_m b \alpha_2 S_m^*}{N_h^*} \implies w_3 = w_4 \frac{\eta \beta_m b \alpha_2 S_m^*}{v_3 N_h^*}, \tag{22}$$

$$w_2 v_2 = w_3 \chi \omega + w_4 \frac{\eta \beta_m b S_m^*}{N_h^*} \implies w_2 = \frac{1}{v_2} \left[w_3 \chi \omega + w_4 \frac{\eta \beta_m b S_m^*}{N_h^*} \right], \tag{23}$$

$$w_5 \mu_m = w_1 \frac{\alpha \beta_h b (S_1^* + \alpha_3 S_2^*)}{N_h^*} \implies w_5 = w_1 \frac{\alpha \beta_h b (S_1^* + \alpha_3 S_2^*)}{\mu_m N_h^*}. \tag{24}$$

Choosing $w_1 = 1$ without loss of generality, we substitute these relations to determine the value of the coefficient for E_h:

$$C_{E_h} = -v_1 + w_2(1-\Phi)\gamma_h + w_3\Phi\gamma_h. \tag{25}$$

From (25), we expand w_2 using (23):

$$\begin{aligned} w_2(1-\Phi)\gamma_h + w_3\Phi\gamma_h &= \frac{(1-\Phi)\gamma_h}{v_2}\left[w_3\chi\omega + w_4\frac{\eta\beta_m b S_m^*}{N_h^*}\right] + w_3\Phi\gamma_h \\ &= w_3\gamma_h\left[\frac{(1-\Phi)\chi\omega}{v_2} + \Phi\right] + w_4\frac{\eta\beta_m b S_m^*(1-\Phi)\gamma_h}{v_2 N_h^*}. \end{aligned} \tag{26}$$

Substituting (22) for w_3:

$$\begin{aligned} &= w_4\frac{\eta\beta_m b\alpha_2 S_m^*}{v_3 N_h^*}\gamma_h\left[\frac{(1-\Phi)\chi\omega}{v_2} + \Phi\right] + w_4\frac{\eta\beta_m b S_m^*(1-\Phi)\gamma_h}{v_2 N_h^*} \\ &= w_4\frac{\eta\beta_m b S_m^*\gamma_h}{N_h^* v_2 v_3}\left[\alpha_2\chi\omega(1-\Phi) + \alpha_2\Phi v_2 + (1-\Phi)v_3\right]. \end{aligned} \tag{27}$$

Now, substituting (21) and (24) for w_4 and w_5 using (27):

$$\begin{aligned} w_4 &= \frac{\gamma_m}{v_6}\cdot\frac{\alpha\beta_h b(S_1^* + \alpha_3 S_2^*)}{\mu_m N_h^*} \\ &= \frac{\alpha\beta_h b(S_1^* + \alpha_3 S_2^*)\gamma_m}{\mu_m v_6 N_h^*}. \end{aligned} \tag{28}$$

Then (26) yields:

$$\begin{aligned} w_2(1-\Phi)\gamma_h + w_3\Phi\gamma_h &= \frac{\alpha\beta_h b(S_1^* + \alpha_3 S_2^*)\gamma_m\eta\beta_m b S_m^*\gamma_h\left[(1-\Phi)v_3 + \chi\omega(1-\Phi)\alpha_2 + \Phi v_2\alpha_2\right]}{\mu_m v_6 v_2 v_3 (N_h^*)^2} \\ &= v_1 R_0^2. \end{aligned} \tag{29}$$

Substituting (29) back into (25), the coefficient of E_h becomes:

$$C_{E_h} = -v_1 + v_1 R_0^2 = v_1(R_0^2 - 1). \tag{30}$$

Now, substituting the equations (21)–(24) and (30)into the derivative of $L(t)$ and using the fact that $S_1 \le S_1^*$, $S_2 \le S_2^*$, and $S_m \le S_m^*$ in the invariant region Ω, we obtain:

$$\begin{aligned} \frac{dL}{dt} \le\ & v_1(R_0^2 - 1)E_h \\ & + \alpha\beta_h b I_m\left[\frac{S_1 + \alpha_3 S_2}{N_h} - \frac{S_1^* + \alpha_3 S_2^*}{N_h^*}\right] \\ & + w_4\eta\beta_m b(A_h + \alpha_2 I_h)\left[\frac{S_m}{N_h} - \frac{S_m^*}{N_h^*}\right]. \end{aligned} \tag{31}$$

Using the properties of the invariant region Ω, since $N_h(t) \ge S_1(t) + S_2(t)$ and $S_1(t) \le S_1^*$, $S_2(t) \le S_2^*$ and $N_h^* = S_1^* + S_2^*$, we have:

$$\frac{S_1 + \alpha_3 S_2}{N_h} \le \frac{S_1 + \alpha_3 S_2}{S_1 + S_2} \le 1, \tag{32}$$

and since $S_m(t) \le S_m^*$, we have:

$$\frac{S_m}{N_h} \le \frac{S_m^*}{N_h^*}. \tag{33}$$

In standard epidemiological formulations, the total population size in the denominator is bounded from below or assumed to be constant at the DFE (i.e., $N_h \approx N_h^*$), which gives:

$$\frac{S_1 + \alpha_3 S_2}{N_h} - \frac{S_1^* + \alpha_3 S_2^*}{N_h^*} \leq 0 \quad \text{and} \quad \frac{S_m}{N_h} - \frac{S_m^*}{N_h^*} \leq 0. \tag{34}$$

Hence, if $R_0 < 1$, then $R_0^2 < 1$, which implies:

$$v_1(R_0^2 - 1)E_h \leq 0, \tag{35}$$

since $v_1 > 0$. Therefore, we conclude that:

$$\frac{dL}{dt} \leq 0 \quad \text{for all } (S_1, S_2, E_h, A_h, I_h, T_h, R_h, S_m, E_m, I_m) \in \Omega. \tag{36}$$

To complete the G.A.S. proof, we identify the largest invariant set where $\frac{dL}{dt} = 0$. Setting $\frac{dL}{dt} = 0$ requires that:

$$v_1(R_0^2 - 1)E_h = 0. \tag{37}$$

Since $R_0 < 1$, the coefficient $v_1(R_0^2 - 1) \neq 0$, which forces:

$$E_h = 0. \tag{38}$$

Substituting $E_h = 0$ into the differential equation (4) for A_h at steady state:

$$\frac{dA_h}{dt} = -v_2 A_h = 0 \implies A_h = 0. \tag{39}$$

Substituting $E_h = 0$ and $A_h = 0$ into the differential equation (5) for I_h:

$$\frac{dI_h}{dt} = -v_3 I_h = 0 \implies I_h = 0. \tag{40}$$

Substituting $I_h = 0$ into the differential equation (6) for T_h:

$$\frac{dT_h}{dt} = -v_4 T_h = 0 \implies T_h = 0. \tag{41}$$

Substituting $T_h = 0$ and $A_h = 0$ into the differential equation (7) for R_h:

$$\frac{dR_h}{dt} = -v_5 R_h = 0 \implies R_h = 0. \tag{42}$$

With $A_h = 0$ and $I_h = 0$, the force of infection for the vectors is:

$$\lambda_m = \frac{\eta \beta_m b(A_h + \alpha_2 I_h)}{N_h} = 0. \tag{43}$$

Substituting $\lambda_m = 0$ into the vector equations (9) and (10) at steady state:

$$\frac{dE_m}{dt} = -v_6 E_m = 0 \implies E_m = 0, \tag{44}$$

$$\frac{dI_m}{dt} = \gamma_m E_m - \mu_m I_m = 0 \implies I_m = 0. \tag{45}$$

Finally, substituting these zero values for all the infected compartments back into the equations for S_1, S_2, and S_m leaves the uninfected linear subsystem:

$$\frac{dS_1}{dt} = \Lambda_h - \rho S_1 + \theta S_2 - \mu_h S_1 = 0, \tag{46}$$

$$\frac{dS_2}{dt} = \rho S_1 - \theta S_2 - \mu_h S_2 = 0, \tag{47}$$

$$\frac{dS_m}{dt} = \Lambda_m - \mu_m S_m = 0. \tag{48}$$

This system has a unique, globally stable equilibrium at (S_1^*, S_2^*, S_m^*). Thus, the largest invariant set contained in $\left\{(S_1, S_2, E_h, A_h, I_h, T_h, R_h, S_m, E_m, I_m) \in \Omega : \frac{dL}{dt} = 0\right\}$ is the singleton $\{E_0\}$.

By LaSalle's Invariance Principle [16], the Disease-Free Equilibrium E_0 is globally asymptotically stable in Ω when $R_0 < 1$.

3.6. Existence of Malaria Endemic Equilibrium Point

The Malaria Endemic Equilibrium Point (MEEP) represents a steady-state solution in which malaria is sustained within the population. The MEEP of the malaria system, denoted as E_1, is expressed as:

$$E_1 = \left(S_1^{**}, S_2^{**}, E_h^{**}, A_h^{**}, I_h^{**}, T_h^{**}, R_h^{**}, S_m^{**}, E_m^{**}, I_m^{**}\right).$$

To find this state, we set all time derivatives in the model to zero. The core of our method is to express all equilibrium state variables as functions of a single reference variable, the exposed human population E_h^{**}.

First, we solve the equilibrium equations for the human asymptomatic, infectious, treated, and recovered populations, such that $\frac{dA_h}{dt} = \frac{dI_h}{dt} = \frac{dT_h}{dt} = \frac{dR_h}{dt} = 0$, we obtain the following:

$$\begin{aligned}
A_h^{**} &= \left(\frac{(1-\Phi)\gamma_h}{\omega+\mu_h}\right) E_h^{**} = C_A E_h^{**},\\
I_h^{**} &= \left(\frac{\Phi\gamma_h + \chi\omega C_A}{\xi+\mu_h+\delta}\right) E_h^{**} = C_I E_h^{**},\\
T_h^{**} &= \left(\frac{\xi C_I}{\alpha_1+\mu_h+\tau}\right) E_h^{**} = C_T E_h^{**},\\
R_h^{**} &= \left(\frac{\tau C_T + (1-\chi)\omega C_A}{\mu_h+\sigma}\right) E_h^{**} = C_R E_h^{**}.
\end{aligned}$$

Next, we determine the total human population at equilibrium. Summing the differential equations for all human compartments reveals the dynamics of the total population N_h, including deaths from treatment failure (α_1):

$$\frac{dN_h}{dt} = \Lambda_h - \mu_h N_h - \delta I_h - \alpha_1 T_h.$$

At equilibrium ($\frac{dN_h}{dt} = 0$), this gives:

$$N_h^{**} = \frac{\Lambda_h - (\delta C_I + \alpha_1 C_T)E_h^{**}}{\mu_h} = N_0 - N_1' E_h^{**},$$

where $N_0 = \frac{\Lambda_h}{\mu_h}$ is the disease-free population size and $N_1' = \frac{\delta C_I + \alpha_1 C_T}{\mu_h}$.

For the vector population, we do not assume that the susceptible vector population is constant. The force of infection on mosquitoes, λ_m^{**}, is:

$$\lambda_m^{**} = \frac{\eta\beta_m b(A_h^{**} + \alpha_2 I_h^{**})}{N_h^{**}} = \frac{K_m E_h^{**}}{N_h^{**}}, \quad \text{where } K_m = \eta\beta_m b(C_A + \alpha_2 C_I).$$

The equilibrium vector populations are then found by solving their respective differential equations set to zero, such that $\frac{dS_m}{dt} = \frac{dE_m}{dt} = \frac{dI_m}{dt} = 0$:

$$\begin{aligned}
S_m^{**} &= \frac{\Lambda_m}{\lambda_m^{**}+\mu_m},\\
E_m^{**} &= \frac{\lambda_m^{**} S_m^{**}}{\gamma_m+\mu_m} = \frac{\Lambda_m \lambda_m^{**}}{(\gamma_m+\mu_m)(\lambda_m^{**}+\mu_m)},\\
I_m^{**} &= \frac{\gamma_m E_m^{**}}{\mu_m} = \frac{\gamma_m \Lambda_m}{(\gamma_m+\mu_m)\mu_m} \cdot \frac{\lambda_m^{**}}{\lambda_m^{**}+\mu_m}.
\end{aligned}$$

This leads to a non-linear expression for the force of infection on susceptible (high-risk) humans, $\lambda_1^{**} = \frac{\alpha\beta_h b I_m^{**}}{N_h^{**}}$:

$$\lambda_1^{**} = \frac{K_{\lambda h} E_h^{**}}{N_h^{**}\left(K_m E_h^{**} + \mu_m N_h^{**}\right)}, \quad \text{where } K_{\lambda h} = \frac{\alpha\beta_h b\gamma_m \Lambda_m K_m}{(\gamma_m+\mu_m)\mu_m}.$$

Finally, the expressions for S_1^{**} and S_2^{**} are found by solving the linear system derived from their respective equilibrium equations given below:

$$S_1^{**} = \frac{Q_1 E_h^{**}(J_2 + \alpha_3 \lambda_1^{**}) + \theta Q_2 E_h^{**}}{(J_1 + \lambda_1^{**})(J_2 + \alpha_3 \lambda_1^{**}) - \rho\theta},$$
$$S_2^{**} = \frac{Q_2 E_h^{**}(J_1 + \lambda_1^{**}) + \rho Q_1 E_h^{**}}{(J_1 + \lambda_1^{**})(J_2 + \alpha_3 \lambda_1^{**}) - \rho\theta},$$

where

$$J_1 = \rho + \mu_h, \quad J_2 = \theta + \mu_h, \quad Q_1 = \Lambda_h + [(1-q)\sigma C_R + zk], \quad Q_2 = [q\sigma C_R + (1-z)k].$$

With respect to the third equation of malaria model equations (1)–(10), when $\frac{dE_h}{dt} = 0$, we get:

$$\lambda_1^{**} S_1^{**} + \alpha_3 \lambda_1^{**} S_2^{**} - (k + \gamma_h + \mu_h) E_h^{**} = 0.$$

By substituting S_1^{**}, S_2^{**}, and λ_1^{**} into the equation above, and after factoring out the disease-free solution $E_h^{**} = 0$, the condition for the endemic equilibrium is given by the roots of a quartic polynomial:

$$P(E_h^{**}) = c_4 (E_h^{**})^4 + c_3 (E_h^{**})^3 + c_2 (E_h^{**})^2 + c_1 E_h^{**} + c_0 = 0.$$

The existence of a biologically meaningful endemic equilibrium depends on this equation having at least one positive real root. The coefficients c_4, c_3, c_2, c_1, and c_0 are complex functions of the model parameters. For completeness and reproducibility, their explicit forms are provided below, constructed from a set of intermediate constants.

Where:

$$\begin{aligned}
c_4 &= z_1 z_2 u_2^2, \\
c_3 &= z_1[2 z_2 u_1 u_2 + z_3 K_m K_{\lambda h} u_2] - K_m K_{\lambda h}[Q_1(J_2 + \alpha_3\rho) + Q_2(\theta + \alpha_3 J_1)]u_2, \\
c_2 &= z_1[z_2(u_1^2 + 2u_0 u_2) + z_3 K_m K_{\lambda h} u_1 + \alpha_3 K_m^2 K_{\lambda h}^2] \\
&\quad - K_m K_{\lambda h}\big(\Lambda_h(J_2 + \alpha_3\rho)u_2 + [Q_1(J_2 + \alpha_3\rho) + Q_2(\theta + \alpha_3 J_1)]u_1\big) \\
&\quad - \alpha_3 K_m^2 K_{\lambda h}^2 [Q_1 + Q_2], \\
c_1 &= z_1[2 z_2 u_0 u_1 + z_3 K_m K_{\lambda h} u_0] \\
&\quad - K_m K_{\lambda h}\big(\Lambda_h(J_2 + \alpha_3\rho)u_1 + [Q_1(J_2 + \alpha_3\rho) + Q_2(\theta + \alpha_3 J_2)]u_0\big) \\
&\quad - \alpha_3 K_m^2 K_{\lambda h}^2 \Lambda_h, \\
c_0 &= z_1 z_2 u_0^2 - K_m K_{\lambda h} \Lambda_h (J_2 + \alpha_3\rho) u_0,
\end{aligned}$$

with intermediate constants:

$$\begin{aligned}
u_2 &= -N_1'(K_m - \mu_m N_1'), \\
u_1 &= N_0(K_m - 2\mu_m N_1'), \\
u_0 &= \mu_m N_0^2, \\
z_1 &= k + \gamma_h + \mu_h, \\
z_2 &= J_1 J_2 - \rho\theta = \mu_h(\rho + \theta + \mu_h), \\
z_3 &= J_2 + \alpha_3 J_1.
\end{aligned}$$

To determine the threshold condition for the existence of a positive endemic equilibrium, we analyze the sign of the constant term c_0. By substituting the definition of $u_0 = \mu_m N_0^2 = \mu_m \left(\frac{\Lambda_h}{\mu_h}\right)^2$ into the expression for c_0, we can factor out positive terms to relate it directly to the basic reproduction number R_0:

$$c_0 = z_1 z_2 u_0^2 \left(1 - \frac{K_m K_{\lambda h} \Lambda_h (J_2 + \alpha_3\rho)}{z_1 z_2 u_0}\right).$$

By comparing this with the expression for R_0 derived in Section 3.3.2, we observe that the term inside the parenthesis is exactly $1 - R_0^2$. Thus, the constant term simplifies to:

$$c_0 = z_1 z_2 u_0^2 (1 - R_0^2).$$

Since all parameters in z_1, z_2, and u_0 are strictly positive, the sign of c_0 is uniquely determined by the threshold parameter R_0:

- $c_0 > 0 \iff R_0 < 1$,
- $c_0 < 0 \iff R_0 > 1$.

The leading coefficient is $c_4 = z_1 z_2 u_2^2$, which is always positive since $z_1, z_2 > 0$ and $u_2^2 \geq 0$. According to Descartes' Rule of Signs, the number of positive real roots of the polynomial $P(E_h^{**}) = 0$ is determined by the number of sign changes in the sequence of its coefficients $(c_4, c_3, c_2, c_1, c_0)$.

When $R_0 > 1$, we have $c_0 < 0$. Since $c_4 > 0$ and $c_0 < 0$, there must be at least one sign change in the sequence of coefficients regardless of the signs of the intermediate coefficients c_3, c_2, and c_1. This mathematically guarantees the existence of at least one positive real root $E_h^{**} > 0$. Once a positive value for E_h^{**} is established, all other endemic state variables $(S_1^{**}, S_2^{**}, A_h^{**}, I_h^{**}, T_h^{**}, R_h^{**}, S_m^{**}, E_m^{**}, I_m^{**})$ are uniquely determined and biologically feasible (non-negative).

Therefore, $R_0 > 1$ is the threshold condition that guarantees the existence of a positive malaria endemic equilibrium.

4 Numerical Simulations/Sensitivity Analysis

In this section, we present numerical simulations and sensitivity analyses of the malaria transmission model (1)–(10) to validate the theoretical findings and evaluate the impact of different control interventions. Simulations were performed using an adaptive 4th/5th-order Runge-Kutta-Fehlberg method (RK45) in Python 3.10 (via the `scipy.integrate.solve_ivp` routine), with an absolute tolerance of 10^{-8} and a time step of $dt = 0.05$ days, over a time domain of $t \in [0, 200]$ days.

The initial conditions used in the simulations are summarized in Table 3. These represent a localized community which corresponds to a total human population of $N_h(0) = 8433$ and a mosquito population of $N_m(0) = 950$. These values represent a localized community or village undergoing a newly introduced epidemic outbreak. The vector population is initialized well below its carrying capacity of $N_m^0 = \frac{\Lambda_m}{\mu_m} \approx 4.5 \times 10^5$, allowing the simulation to capture transient ecological feedback and vector growth dynamics.

The baseline parameter values are listed in Table 4, gathered and justified from standard malaria literature [20, 11, 2, 4, 21, 22, 23].

Table 3: State Variables and Their Initial Values

Variable	Initial Value	Justification / Description
$S_1(0)$	5600	High-risk susceptible population (low awareness)
$S_2(0)$	1500	Low-risk susceptible population (high awareness)
$E_h(0)$	1000	Exposed humans (latent reservoir)
$A_h(0)$	0	Initial asymptomatic carriers
$I_h(0)$	320	Symptomatic infectious humans (active outbreak)
$T_h(0)$	10	Initial treated individuals
$R_h(0)$	3	Initial recovered individuals
$S_m(0)$	600	Susceptible vector population
$E_m(0)$	150	Exposed vector population
$I_m(0)$	200	Infectious vector population

Table 4: Parameters and Their Values

Parameter	Baseline Value (Range)	Unit	Source
Λ_h	90	day^{-1}	[11]
Λ_m	5000	day^{-1}	Assumed
θ	0.01	day^{-1}	Assumed
ρ	0.01	day^{-1}	Assumed
Φ	0.3	dimensionless	[2]
ω	0.09	day^{-1}	Assumed (average asymptomatic duration $\approx$ 11 days)
γ_h	0.35	day^{-1}	[2]
ξ	0.17	day^{-1}	[2]
q	0.7	dimensionless	Assumed
σ	0.00556	day^{-1}	[2]
α_3	0.2 (0.2–0.9)	dimensionless	Assumed (efficacy range of bed nets)
γ_m	0.061551	day^{-1}	[11]
α_2	0.7	dimensionless	Assumed
α	0.5	dimensionless	Assumed
β_h	0.3	day^{-1}	Assumed
β_m	0.1	day^{-1}	Assumed
b	0.5	day^{-1}	Assumed
η	0.5	dimensionless	Assumed
μ_h	4.089×10^{-5}	day^{-1}	[1] (life expectancy $\approx$ 67 years)
μ_m	0.0111111	day^{-1}	[1] (mosquito lifespan $\approx$ 90 days)
δ	0.08	day^{-1}	Assumed
z	0.001910	dimensionless	[11]
k	0.115671	day^{-1}	[11]
χ	0.2	dimensionless	Assumed
α_1	0.006	day^{-1}	[2]
τ	0.00475	day^{-1}	[2]

4.1 Sensitivity Analysis

We applied Latin Hypercube Sampling (LHS) and Partial Rank Correlation Coefficient (PRCC) analysis using Python 3.10 with the `scipy.stats` package to quantify the sensitivity of the reproduction number R_0 to changes in the model parameters. Parameter ranges were defined within $\pm 25\%$ of their baseline values under a uniform distribution. The resulting PRCC values are summarized in Table 5 and illustrated in Figure 2.

The sensitivity indices reveal that the two most influential parameters are the mosquito biting rate (b, PRCC = $+0.93$) and the mosquito natural death rate (μ_m, PRCC = -0.94). Other parameters that significantly increase R_0 include transmission probabilities (β_h, β_m) and vector density (Λ_m). Conversely, interventions that effectively reduce R_0 include the progression rate of asymptomatic individuals (ω, PRCC = -0.73), the treatment rate (ξ, PRCC = -0.11), and the awareness rate (ρ, PRCC = -0.37). This analysis strongly suggests that vector control campaigns aimed at increasing mosquito mortality (e.g., IRS, LLINs) remain the most effective interventions, but behavioural campaigns (ρ) and active case screening (ω) are crucial secondary modulators.

4.2 Model Simulation

In this section, we present numerical simulations to support our analytical results. By varying the progression rate (ω) and the awareness participation rate (ρ), we simulated three distinct epidemiological scenarios:

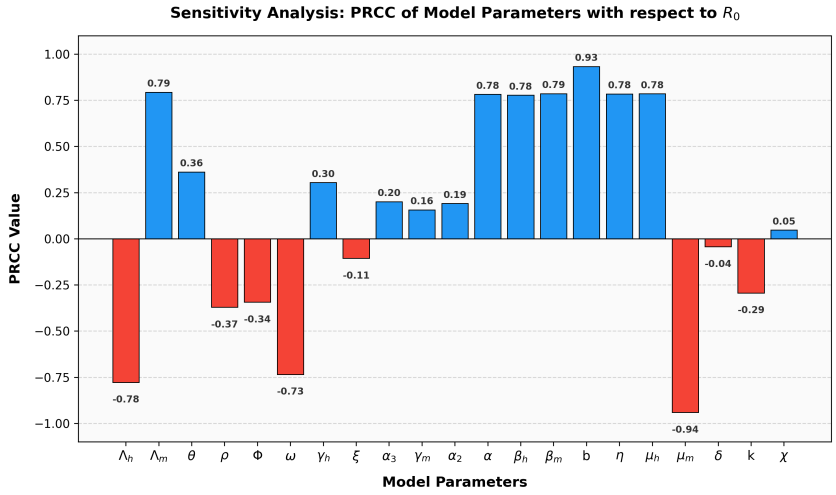

Figure 2: Bar graph illustrating the partial rank correlation coefficients (PRCC) of the model parameters with respect to the basic reproduction number R_0.

Table 5: Partial Rank Correlation Coefficients (PRCC) and LHS Sampling Ranges of Parameters with Respect to R_0

Parameter	LHS Sampling Range ($\pm 25\%$)	PRCC Value	Significance / Direction
Λ_h	$[67.5,\ 112.5]$	-0.7774	Negative (Population dilution effect)
Λ_m	$[3750,\ 6250]$	$+0.7935$	Positive (Vector density increase)
θ	$[0.0075,\ 0.0125]$	$+0.3614$	Positive (Forgetfulness increases susceptibility)
ρ	$[0.0075,\ 0.0125]$	-0.3711	Negative (Awareness reduces transmission)
Φ	$[0.225,\ 0.375]$	-0.3436	Negative (Symptomatic progression reduces reservoir)
ω	$[0.0675,\ 0.1125]$	-0.7345	Negative (Asymptomatic clearance/clinical progression)
γ_h	$[0.2625,\ 0.4375]$	$+0.3043$	Positive (Host progression increase)
ξ	$[0.1275,\ 0.2125]$	-0.1058	Negative (Symptomatic treatment reduces pool)
α_3	$[0.15,\ 0.25]$	$+0.2011$	Positive (LLIN failure increases risk)
γ_m	$[0.046163,\ 0.076939]$	$+0.1567$	Positive (Vector progression rate)
α_2	$[0.525,\ 0.875]$	$+0.1907$	Positive (Symptomatic infectiousness)
α	$[0.375,\ 0.625]$	$+0.7820$	Positive (Human risk modifier)
β_h	$[0.225,\ 0.375]$	$+0.7771$	Positive (Vector-to-host transmission)
β_m	$[0.075,\ 0.125]$	$+0.7855$	Positive (Host-to-vector transmission)
b	$[0.375,\ 0.625]$	$+0.9324$	Positive (Biting rate - most influential)
η	$[0.375,\ 0.625]$	$+0.7845$	Positive (Host-to-vector transmission contact)
μ_h	$[3.067 \times 10^{-5},\ 5.111 \times 10^{-5}]$	$+0.7848$	Positive (Human mortality influence)
μ_m	$[0.008333,\ 0.013889]$	-0.9412	Negative (Mosquito mortality - most effective reduction)
δ	$[0.06,\ 0.10]$	-0.0436	Negative (Disease-induced death removes carriers)
k	$[0.086753,\ 0.144589]$	-0.2937	Negative (Immune recovery reduces exposed)
χ	$[0.15,\ 0.25]$	$+0.0467$	Positive (Progression fraction to symptomatic)

1. **High-Awareness/Screening Case** ($R_0 \approx 0.58$)**:** We set $\omega = 0.9$ and $\rho = 0.2$. This represents an aggressive campaign with rapid case detection and behavioral change. The system converges to the disease-free equilibrium (DFE), and the infection is successfully eradicated (Figures 3a and 4a).

2. **Baseline Outbreak Case** ($R_0 \approx 1.96$)**:** We set the parameters to their baseline values ($\omega = 0.09$ and $\rho = 0.01$). Here, $R_0 > 1$, and the system experiences an epidemic wave before converging to a stable endemic state, showing persistent disease transmission (Figures 3b and 4b).

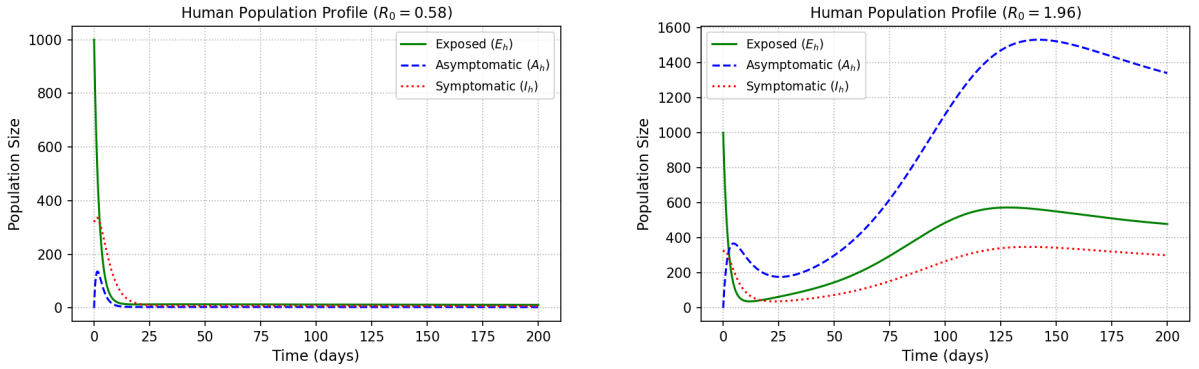

(a) $R_0 \approx 0.58$ (b) $R_0 \approx 1.96$

Figure 3: Dynamic profiles of human disease compartments (Exposed E_h, Asymptomatic A_h, Symptomatic I_h) under the two scenarios.

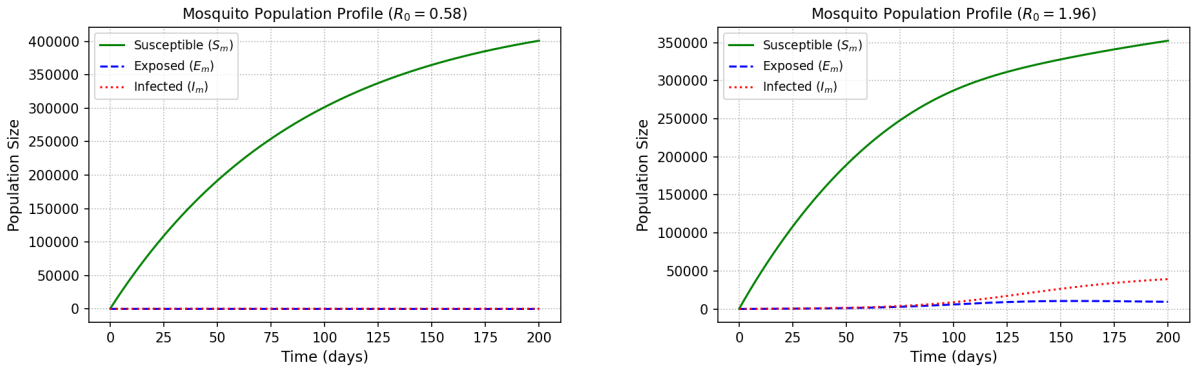

(a) $R_0 \approx 0.58$ (b) $R_0 \approx 1.96$

Figure 4: Dynamic profiles of vector compartments (Susceptible S_m, Exposed E_m, Infected I_m) under the two scenarios.

4.3 The Effect of Model Parameters

We now explore the individual and combined effects of key parameters on transmission dynamics.

4.3.1 Varying the LLIN failure rate (α_3)

Figures 5a–5d illustrate how the net inefficacy factor (α_3) affects the compartments, keeping other parameters constant. Low net failure ($\alpha_3 = 0.05$) reduces transmission, leading to low numbers of asymptomatic hosts, symptomatic hosts, and infected mosquitoes. Conversely, a failing bed net program ($\alpha_3 = 0.8$) causes a major increase in all infected compartments, demonstrating that net quality and usage rates are paramount to malaria control.

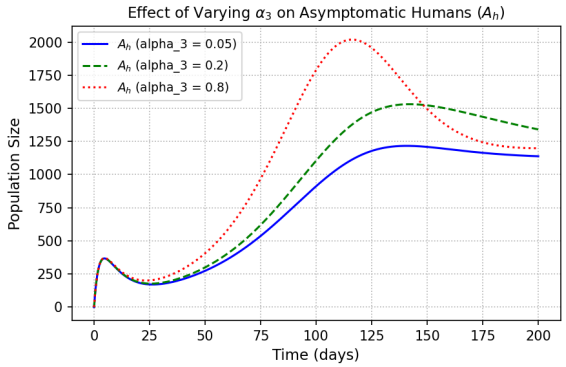

(a) Asymptomatic A_h

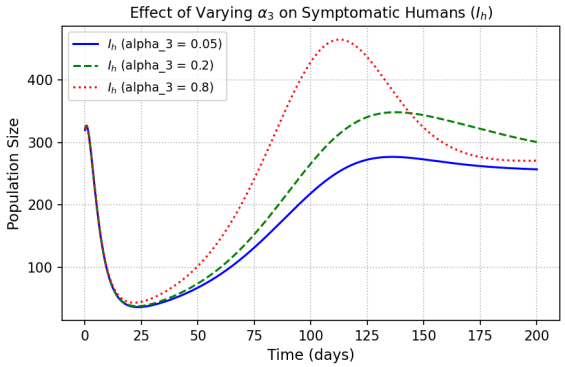

(b) Symptomatic I_h

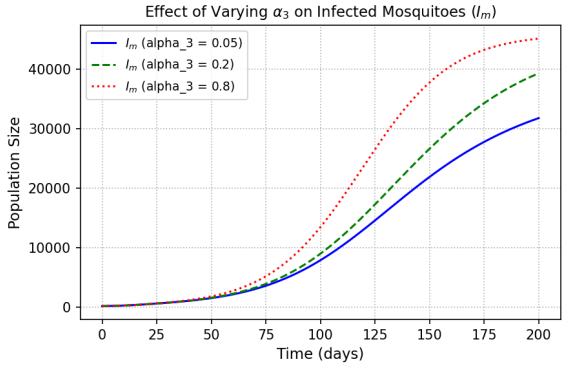

(c) Infected vectors I_m

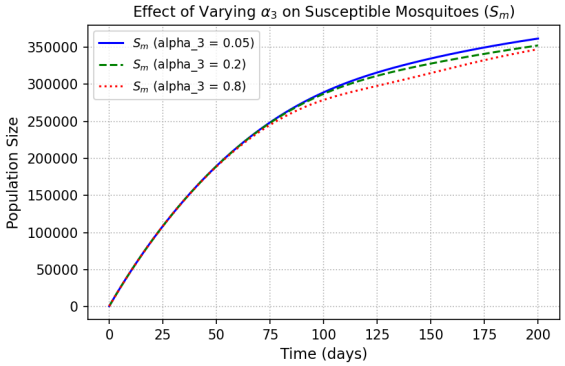

(d) Susceptible vectors S_m

Figure 5: Impact of varying LLIN failure rate α_3 on human and vector compartments.

4.3.2 Varying the asymptomatic progression rate (ω)

Figures 6a and 6b show the effect of varying the progression rate ω on the asymptomatic (A_h) and symptomatic (I_h) human classes. Increasing ω (which represents accelerated case detection and clinical progression of asymptomatic carriers) reduces the asymptomatic pool and decreases the overall endemic prevalence. Conversely, low progression ($\omega = 0.02$) allows asymptomatic carriers to persist for longer, sustaining transmission.

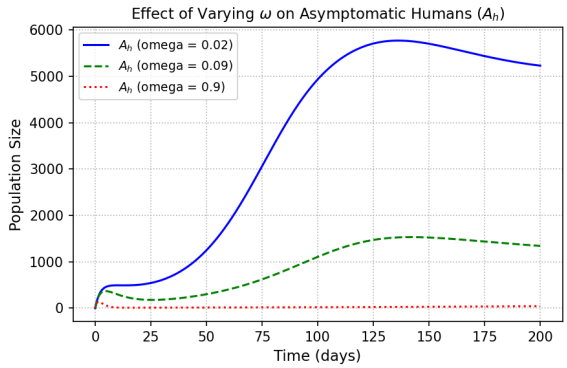

(a) Asymptomatic A_h

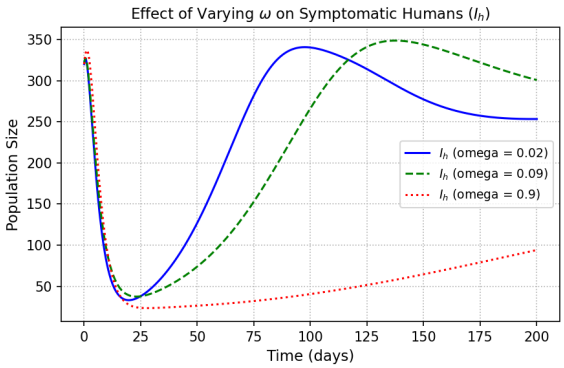

(b) Symptomatic I_h

Figure 6: Impact of varying asymptomatic progression rate ω on human compartments.

4.3.3 Varying the awareness participation rate (ρ)

Figures 7a–7d show that increasing the rate of awareness participation (ρ) shifts the susceptible human population from the high-risk class (S_1) to the low-risk class (S_2). This leads to a major reduction in asymptomatic hosts, symptomatic hosts, and infected vectors, confirming that behavioural campaigns are highly effective tools.

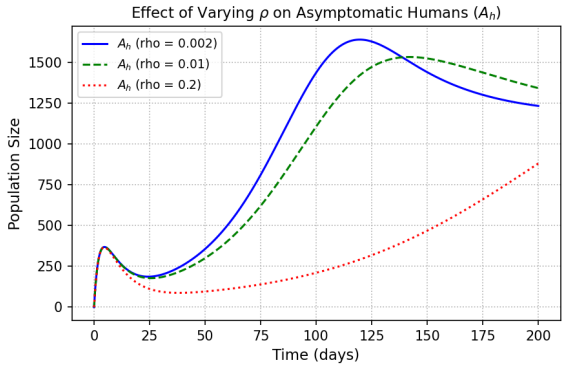

(a) Asymptomatic A_h

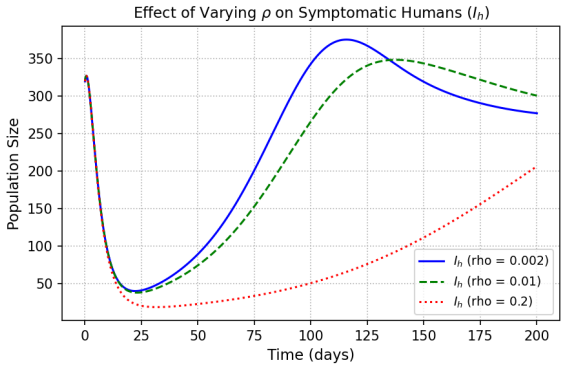

(b) Symptomatic I_h

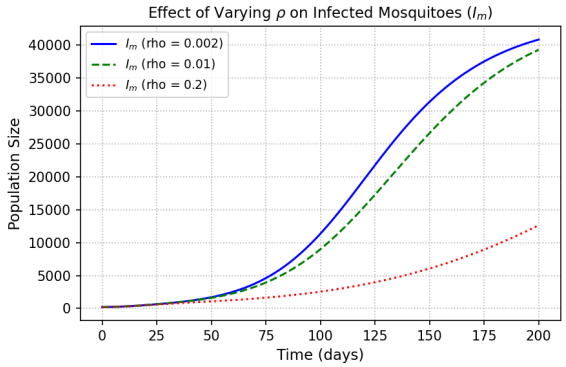

(c) Infected vectors I_m

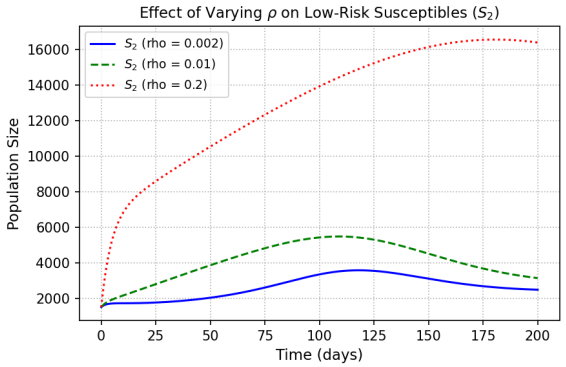

(d) Low-risk susceptibles S_2

Figure 7: Impact of varying awareness participation rate ρ on human and vector compartments.

4.3.4 Varying the forgetfulness rate (θ)

Figures 8a–8d show that an increase in the forgetfulness rate θ causes individuals in the low-risk class S_2 to lose awareness and return to the high-risk class S_1. This wanes the impact of behavioral campaigns and increases all infected compartments, demonstrating that awareness campaigns must be sustained periodically to prevent behavioral relapse.

4.3.5 Varying the treatment rate (ξ)

Figures 9a and 9b illustrate that increasing the treatment rate ξ of symptomatic hosts shrinks both the symptomatic (I_h) and asymptomatic (A_h) pools. This highlights an indirect community feedback loop: treating symptomatic cases prevents vectors from feeding on infected hosts, which lowers the force of infection and subsequently reduces new asymptomatic cases.

4.4 The Role of Asymptomatic Infection

4.4.1 Dependency of Asymptomatic Infection on Parameters

To evaluate the long-term dependency of the asymptomatic reservoir on key biological and intervention parameters, we performed steady-state grid simulations to generate 3D parameter space surfaces (Figures

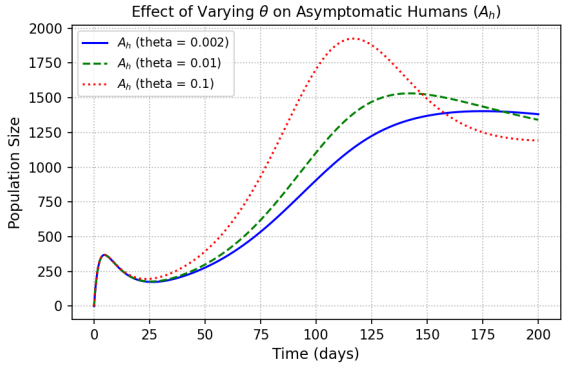

(a) Asymptomatic A_h

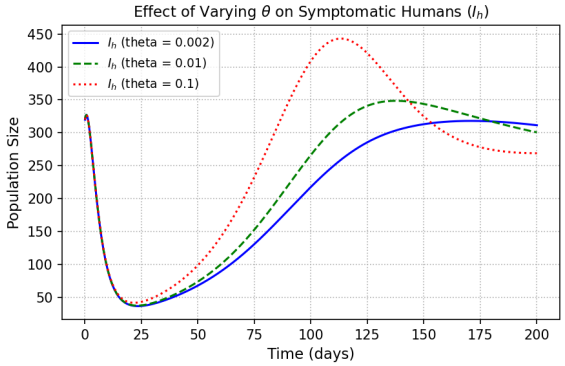

(b) Symptomatic I_h

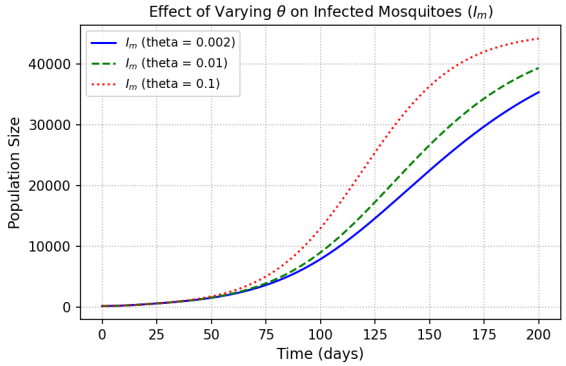

(c) Infected vectors I_m

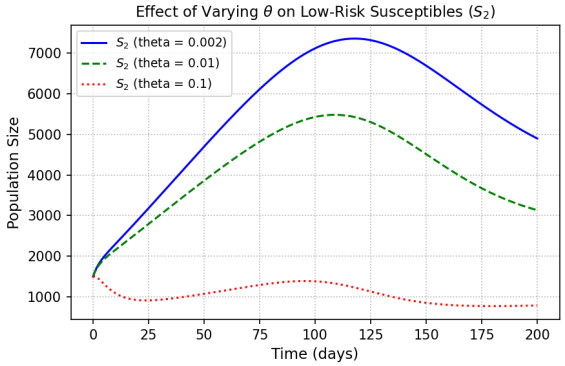

(d) Low-risk susceptibles S_2

Figure 8: Impact of varying forgetfulness rate θ on human and vector compartments.

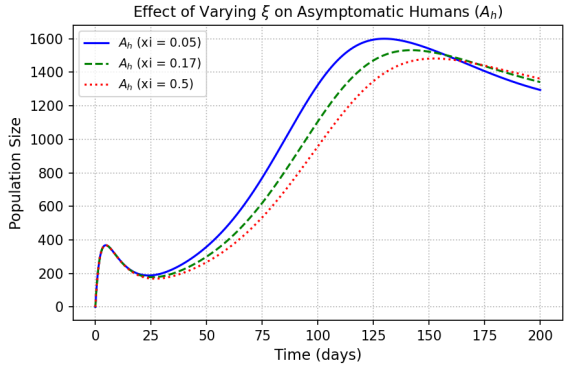

(a) Asymptomatic A_h

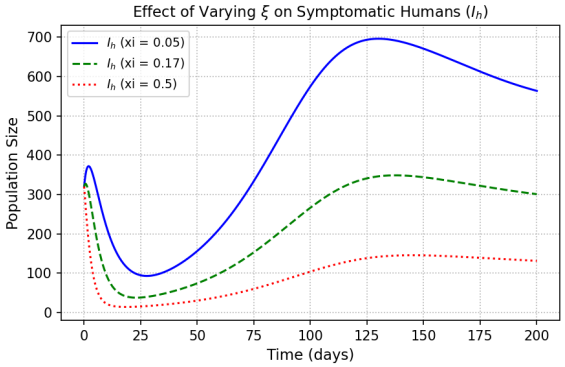

(b) Symptomatic I_h

Figure 9: Impact of varying treatment rate ξ on human compartments.

10a–10c).

- **Figure 10a** (ω **vs.** α_3)**:** The parameter space reveals a sharp, cliff-like threshold driven by the LLIN failure rate (α_3). When α_3 is low ($\alpha_3 < 0.5$), the asymptomatic prevalence (A_h) is entirely suppressed, remaining in the dark blue "safe zone" ($A_h \approx 0$). As α_3 crosses this critical threshold, A_h surges to form a high-prevalence plateau (red zone). The progression rate ω acts as a secondary modulator; peak prevalence occurs where $\alpha_3 \to 1$ and $\omega \to 0$. This shows that successful vector control (α_3) overrides natural disease progression.

- **Figure 10b** (ω **vs.** ξ)**:** The peak asymptomatic prevalence (deep red) is at the origin ($\omega \to 0, \xi \to 0$), representing a worst-case scenario where asymptomatic carriers do not progress to symptoms and clinical treatment is absent. Increasing clinical treatment (ξ) causes a steep drop in A_h, proving that treating clinical malaria has strong indirect community protective effects. High ω and high ξ act synergistically to drain the asymptomatic reservoir rapidly.

- **Figure 10c** (ρ **vs.** ω)**:** This surface maps behavioural campaigns (ρ) against progression (ω). The asymptomatic population surges into an "epidemic wall" (red spike) only at the extreme corner where the awareness rate is near zero ($\rho \approx 0$). Achieving just a small, critical mass of behavioral change ($\rho \geq 0.05$) triggers a rapid collapse of the asymptomatic reservoir, demonstrating the high return on investment for public health education campaigns.

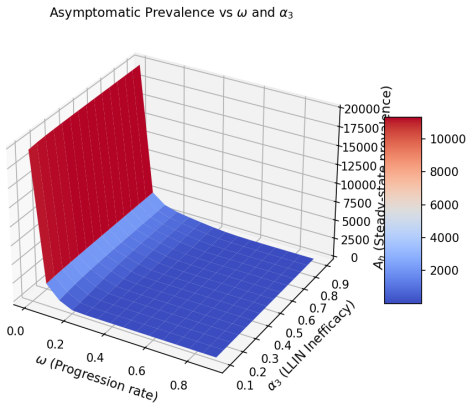

(a) A_h vs. ω and α_3

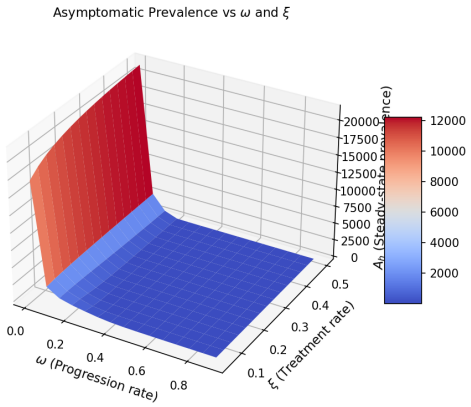

(b) A_h vs. ω and ξ

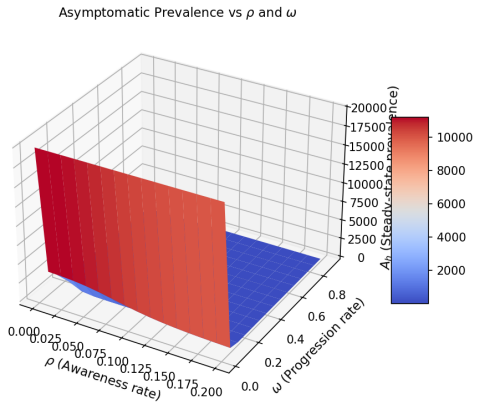

(c) A_h vs. ρ and ω

Figure 10: 3D surface plots illustrating steady-state asymptomatic prevalence (A_h) under varying parameter pairs.

4.4.2 Asymptomatic Infection Contribution to R_0

The analytical expression of the reproduction number R_0 derived in Section 3.3.2 can be decomposed into distinct asymptomatic (R_{0A}) and symptomatic (R_{0I}) transmission loops:

$$R_0 = \sqrt{R_{0A}^2 + R_{0I}^2}. \tag{49}$$

The symptomatic factor is given by $\alpha_2\Phi(\mu_h+\omega)$ and the asymptomatic factor is $(1-\Phi)(\alpha_2\chi\omega+\mu_h+\xi+\delta)$ in the numerator of the next-generation matrix terms. Applying the baseline parameter values from Table 4, the numerical values of these factors are computed as:

$$\begin{aligned} N_A &= (1-\Phi)\left[\alpha_2\chi\omega+\mu_h+\xi+\delta\right] \approx 0.183849, \\ N_I &= \alpha_2\Phi(\mu_h+\omega) \approx 0.018909. \end{aligned}$$

Comparing the relative ratios of these factors:

$$\begin{aligned} \text{Asymptomatic Loop Contribution} &= \frac{N_A}{N_A+N_I} \times 100\% \approx 90.7\%, \\ \text{Symptomatic Loop Contribution} &= \frac{N_I}{N_A+N_I} \times 100\% \approx 9.3\%, \end{aligned}$$

This reveals that the asymptomatic class contributes approximately 90.7% to the transmission threshold, while the symptomatic class accounts for only 9.3%. This indicates that, for the parameter values used, the contribution of symptomatic individuals to the spread of the disease is almost negligible. This could be because they are quickly identified and treated (a high ξ) or die (a high δ), effectively removing them from the transmitting population very quickly. Meanwhile, asymptomatic individuals, while they may recover slowly (a low ω), persist long enough to be responsible for virtually all new infections.

Increasing the progression rate to $\omega = 0.9$ and the awareness participation rate to $\rho = 0.2$ decreases the asymptomatic contribution to 57.0%, while increasing the symptomatic contribution to 43.0%. However, it was observed that increasing only ρ to 0.2 didn't have much effect in reducing the pool of the asymptomatic class. This tells us that awareness alone is insufficient for malaria elimination; behavioural campaigns must be coupled with active case detection, diagnostic screening, and effective treatment to drain the asymptomatic reservoir and achieve malaria eradication.

5 Conclusion

This study developed and analysed a comprehensive malaria transmission model that integrates awareness dynamics with the epidemiological role of asymptomatic carriers, addressing a critical gap in the existing modelling literature. By stratifying the susceptible population into high-risk and low-risk groups based on awareness level and incorporating an explicit asymptomatic class, the model captures both behavioural and biological drivers of transmission.

The analytical results demonstrate that the malaria-free equilibrium is locally and globally asymptotically stable when the basic reproduction number $R_0 < 1$, but the persistence of asymptomatic infections substantially broadens the parameter region where malaria remains endemic. Sensitivity analysis further shows that awareness-related parameters interact strongly with biological transmission processes, highlighting the importance of considering both behavioural and epidemiological mechanisms when designing control strategies.

While the model provides valuable insights, it is built on several simplifying assumptions that can be addressed in future research. The assumption of homogeneous mixing overlooks spatial heterogeneity and human mobility, which are known to influence transmission patterns through importation and local clustering. Diagnostic limitations and submicroscopic infections are not explicitly represented, potentially overstating the effectiveness of surveillance.

Despite these limitations, the integrated awareness–asymptomatic framework presented here represents a significant advancement over models that consider these processes separately. The major implication is clear: awareness-based behavioural change enhances the impact of biomedical interventions, but in regions where asymptomatic infections are prevalent, awareness alone cannot eliminate malaria. Effective control requires combined strategies that simultaneously reduce exposure, promote early treatment, and identify or treat hidden reservoirs of infection. Incorporating additional layers of realism, such as spatial structure, seasonality, diagnostic sensitivity, heterogeneity in behaviour, and cost-effectiveness, would further strengthen the model's applicability to real-world malaria control planning.

Declaration

Competing Interest

The authors declare that they have no competing interest.

Author Contributions

All authors contributed to the design, analysis, simulations, and writing of the paper.

Funding

This study received no external funding.

Availability of Data and Material

All data and parameters used in the study are included in the manuscript.

Acknowledgement

The authors would like to thank the anonymous reviewers for their valuable suggestions and feedback, which have greatly helped to improve the clarity of the original manuscript. The first author would like to acknowledge support from the ICTP through the Associates Programme (2026-2031).

References

[1] World Health Organization (2025). *World malaria situation update: Global malaria report*. Technical report, WHO Online.

[2] Haringo, A. T., Obsu, L. L., and Bushu, F. K. (2025). Impact of asymptomatic infections on malaria transmission dynamics. *Infectious Disease Modelling*, 10:1456–1478.

[3] Haile, G. T., Koya, P. R., and Legesse, F. M. (2025). Sensitivity analysis of a mathematical model for malaria transmission accounting for infected ignorant humans and relapse dynamics. *Frontiers in Applied Mathematics and Statistics*, 10:11234.

[4] Xue, R. et al. (2023). A malaria transmission model with asymptomatic infection: Global dynamics and intervention analysis. *Journal of Theoretical Biology*, 564:111520.

[5] Jaleta, S. F. et al. (2025). Mathematical modelling and optimal control with symptomatic and asymptomatic carriers. *Frontiers in Applied Mathematics and Statistics*, 11:1245.

[6] Rek, J. et al. (2022). Asymptomatic school-aged children are important drivers of malaria transmission. *The Journal of Infectious Diseases*, 225:128–137.

[7] Mandai, S. S. et al. (2024). High prevalence and risk of malaria among asymptomatic individuals from villages with high prevalence of artemisinin partial resistance in kyerwa district of kagera region, north-western tanzania. *Malaria Journal*, 23:197.

[8] Collins, O. C. and Duffy, K. J. (2022). A mathematical model for the dynamics and control of malaria in nigeria. *Infectious Disease Modelling*, 7:452–469.

[9] Adegbite, G., Edeki, S., Isewon, I., Emmanuel, J., Dokunmu, T., Rotimi, S., Oyelade, J., and Adebiyi, E. (2023). Mathematical modeling of malaria transmission dynamics in humans with mobility and control states. *Infectious Disease Modelling*, 8:1015–1031.

[10] Al Basir, F. and Abraha, T. (2023). Mathematical modelling and optimal control of malaria using awareness-based interventions. *Mathematics*, 11:1687.

[11] Ochieng, F. O. (2023). Seirs model for malaria transmission dynamics incorporating seasonality and awareness campaign. *Infectious Disease Modelling*, 9:84–102.

[12] Haringo, A. T., Obsu, L. L., and Bushu, F. K. (2024). A mathematical model of malaria transmission with media-awareness and treatment interventions. *Journal of Applied Mathematics and Computing*, 70:4715–4753.

[13] Diekmann, O., Heesterbeek, J. A. P., and Metz, J. A. J. (1990). On the definition and the computation of the basic reproduction ratio r0 in models for infectious diseases in heterogeneous populations. *Journal of Mathematical Biology*, 28:365–382.

[14] Van den Driessche, P. and Watmough, J. (2002). Reproduction numbers and sub-threshold endemic equilibria for compartmental models of disease transmission. *Mathematical Biosciences*, 180(1–2):29–48.

[15] Castillo-Chavez, C. and Song, B. (2004). Dynamical models of tuberculosis and their applications. *Mathematical Biosciences and Engineering*, 1(2):361–404.

[16] LaSalle, J. P. (1976). *The Stability of Dynamical Systems*. Regional Conference Series in Applied Mathematics, SIAM, Philadelphia, PA.

[17] Shuai, Z. and van den Driessche, P. (2013). Global stability of infectious disease models using Lyapunov functions. *Journal of Mathematical Biology*, 66:1513–1522.

[18] Lakshmikantham, V., Leela, S., and Martynyuk, A. A. (1989). *Stability Analysis of Nonlinear Systems*. Marcel Dekker, New York.

[19] Smith, H. L. (1995). *Monotone Dynamical Systems: An Introduction to the Theory of Competitive and Cooperative Systems*. American Mathematical Society, Providence, RI.

[20] Chitnis, N., Hyman, J. M., and Cushing, J. M. (2008). Determining important parameters in the spread of malaria through the sensitivity analysis of a mathematical model. *Bulletin of Mathematical Biology*, 70:1272–1296.

[21] Bousema, T., Okell, L., Felger, I., and Drakeley, C. (2014). Asymptomatic malaria infections: detectability, transmissibility and public health relevance. *Nature Reviews Microbiology*, 12(12):833–840.

[22] Lindblade, K. A., Steinhardt, L., Samuels, A., and Slutsker, L. (2015). The contribution of asymptomatic and submicroscopic parasite carriers to transmission in endemic areas. *Malaria Journal*, 14:223.

[23] Marino, S., Hogue, I. B., Ray, C. J., and Kirschner, D. E. (2008). A methodology for performing global uncertainty and sensitivity analysis in systems biology. *Journal of Theoretical Biology*, 254(1):178–196.

[24] Aguilar, J. et al. (2020). Mathematical analysis of malaria models including asymptomatic infections. *Mathematical Biosciences and Engineering*, 17:3412–3428.

[25] Collins, O. C. and Duffy, K. J. (2020). Estimating the impact of lock-down, quarantine and sensitization in a covid-19 outbreak: lessons from the covid-19 outbreak in china. *PeerJ*, 8:e9933.

[26] Febiriana, E. et al. (2024). Exploring the interplay between social awareness and the use of bed nets in a malaria control program. *Infectious Disease Modelling*, 9:112–128.

[27] Kim, J. E., Choi, Y., and Lee, C. H. (2019). Effects of climate change on plasmodium vivax malaria transmission dynamics: A mathematical modeling approach. *Applied Mathematics and Computation*, 347:616–630.

[28] Mwebesa, E. et al. (2024). Impact of mass-media malaria campaigns on knowledge and preventive behaviour among pregnant women. *BMC Public Health*, 24:128.

[29] Okuneye, K. and Gumel, A. B. (2017). Analysis of a temperature-and rainfall-dependent model for malaria transmission dynamics. *Mathematical Biosciences*, 287:72–92.

[30] Ozodiegwu, I. D. et al. (2023). Evaluating nigeria's national malaria strategic plan through model-based analysis. *Malaria Journal*, 22:54.

[31] Ross, R. (1911). *The prevention of malaria*. John Murray, London.

[32] Talabi, F. et al. (2024). Radio messages and malaria preventive practices in malaria-endemic regions: Evidence from community radio campaigns. *International Journal of Environmental Research and Public Health*, 21:341.

[33] Tchoumi, K. M., Banasiak, J., and Ouifki, R. (2025). A meta-population malaria model with migration, screening, and asymptomatic reservoirs. *Journal of Biological Systems*, 33:145–172.